nature portfolio

https://doi.org/10.1038/s41559-021-01486-0

Supplementary information

Ecological factors influence balancing selection on leaf chemical profiles of a wildflower

In the format provided by the authors and unedited

Supplementary Information

supporting

“Ecological factors influence balancing selection on leaf chemical profiles of a wildflower**”**
Lauren N. Carley *et al.*

Contents:

Supplementary figures

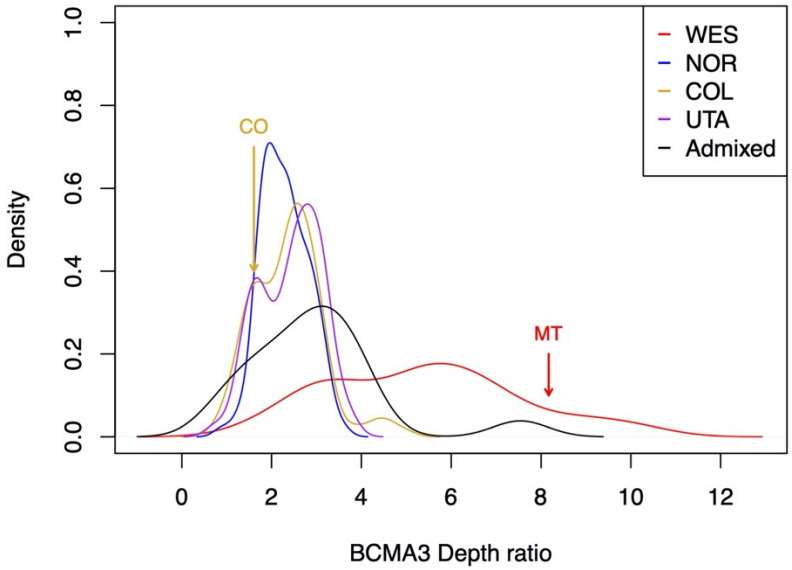

Supplementary Figure 1. Gene duplication and loss events yield variable BCMA copy number across genetic groups and accessions. Colored lines indicate the distribution of estimated *BCMA* copy number for population groups as characterized in Wang et al. (2019), determined by read depth of genomic sequence data (Supplementary Methods). Arrows indicate the distribution of estimated copy number, for parental genotypes used to generate CFR-NILs: CO (SAD; gold) and MT (LTM; red).

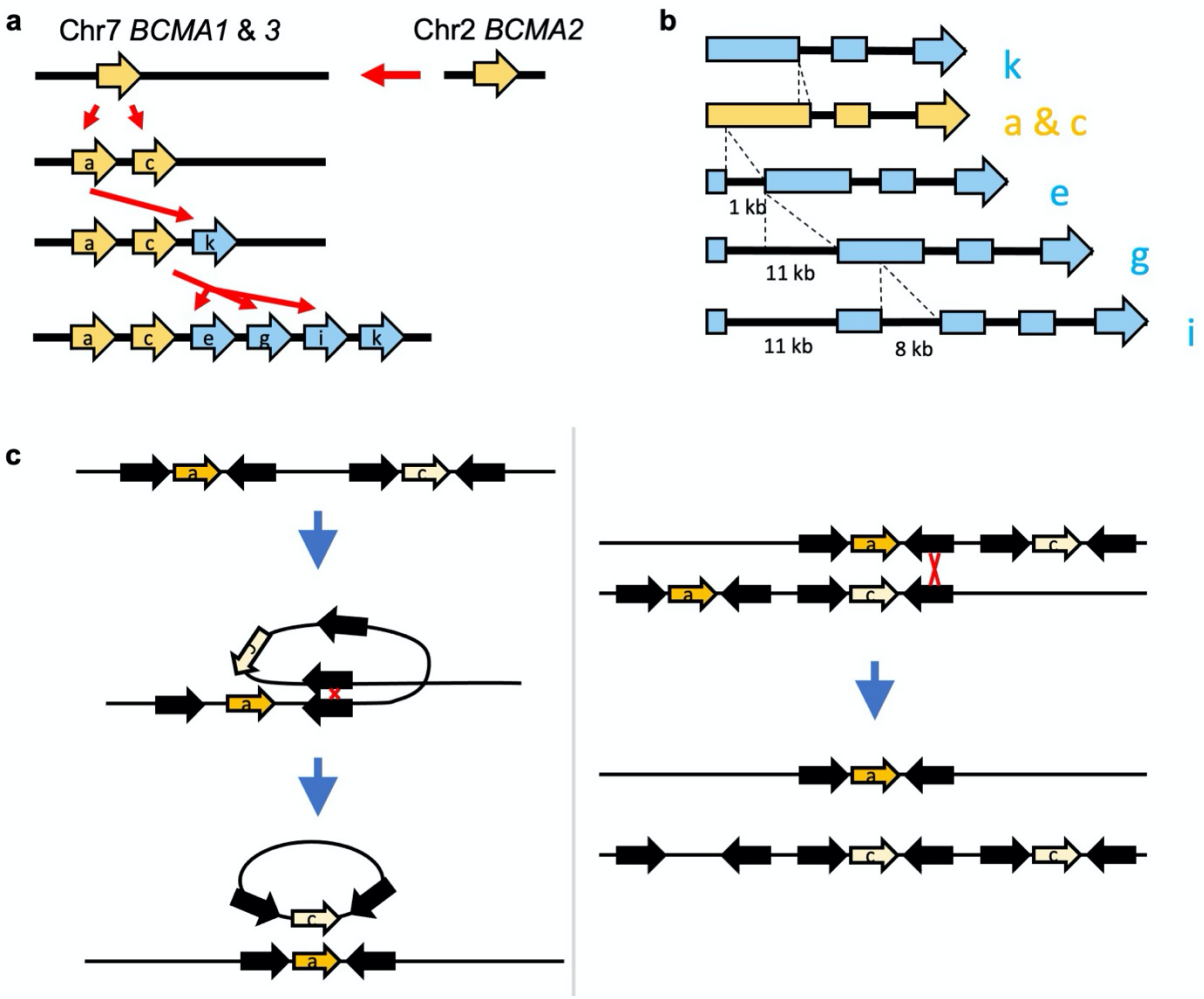

Supplementary Figure 2. Inferred evolutionary history of *BCMA* duplications in *B. stricta*. (a) Following the initial duplication event from chromosome 2 to chromosome 7, *BCMA1/3* was copied several more times, with both *BCMAa* (*BCMA3*) and *BCMAc* (*BCMA1*) yielding progeny copies (labels following Extended Data Figure 5). (b) Sequence alignment reveals insertions and deletions that convert most gene copies into non-functional pseudogenes, leaving high copy number in the LTM parent. (c) Proposed mechanisms causing the secondary loss of *BCMA1*, as in the SAD12 (CO CFR-NIL parental) genotype. Due to the prevalence of repetitive elements in the BCMA region on chromosome 7, it is possible that recombination events among inverted repeats (visible in Extended Data Figure 7) excised *BCMA1* from some genetic backgrounds, either within a chromosome (left) or during crossing-over among chromosomes (right). The latter scenario could also contribute to the proliferation of the *BCMA* pseudogenes and flanking elements present in some lineages (see Extended Data Figures 5 and 7).

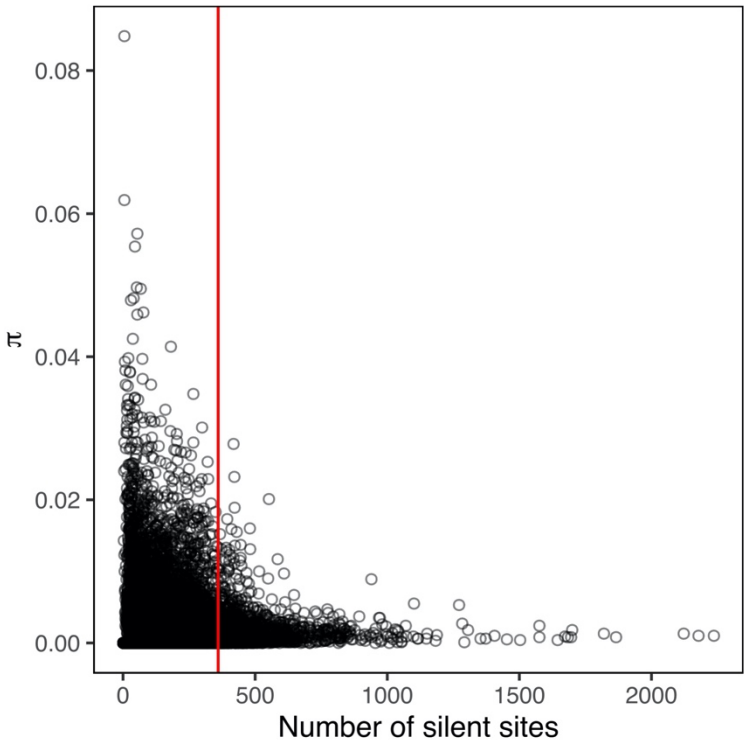

Supplementary Figure 3. Nucleotide diversity is negatively correlated with gene size. Each point represents one gene in the *B. stricta* genome for which π data was calculable and greater than 0 among a subset of 54 genotypes (see Supplementary Methods). Levels of nucleotide diversity (π) are highest for genes with few silent sites. To account for this, we compared π_{BCMA} to π of genes across the genome with a similar number of silent sites. *BCMA3* contains 364 silent sites, so our threshold was 360 (indicated by red line).

Supplementary tables

Supplementary Table 1. Variation in damage across *BCMA1/3* CFR-NIL genotypes in manipulative arrays in six field environments (**A**), permanent transplants in nine field environments (**B**), and one lab environment using the model herbivore *Trichoplusia ni* (Lepidoptera: Noctuidae) (**C**).

Model term	Satterthwaite's method				Kenward-Roger's method			
	DF (num, den)	Test statistic†	*P*		DF (num, den)	Test statistic†	*P*	
A) Temporary arrays (N = 5,193)								
BCMA1/3	1, 9.201	8.3990	0.0173	*	1, 9.0	8.3990	0.01767	*
Environment	5, 48.74	2.2721	0.0618	.	5, 52.0	2.2721	0.06077	.
BCMA1/3×Env	5, 5149	2.3623	0.0376	*	5, 5150.0	2.3623	0.03761	*
Frequency‡	2, 49.07	0.7569	0.4745		2, 52.3	0.7569	0.47418	
BCMA1/3×Frequency‡	2, 5119	0.6312	0.5320		2, 5121.5	0.6312	0.53198	
Block§	1	530.21	<.0001	***	1	530.21	<.0001	***
CFR-NIL family line§	1	1.98	0.1597		1	1.98	0.1597	
B) Permanent transplants (N = 3,674)								
BCMA1/3	1, 15.77	0.0934	0.7639		1, 15.96	0.0935	0.7638	
Environment	8, 140.7	28.0465	<.0001	***	8, 135.15	28.0462	<.0001	***
BCMA1/3×Env	8, 2835	4.1880	<.0001	***	8, 2840.39	4.1884	<.0001	***
Block§	1	356.91	<.0001	***	1	356.91	<.0001	***
CFR-NIL family line§	1	16.80	<.0001	***	1	16.80	<.0001	***
C) Laboratory environment (N = 214)								
BCMA1/3	1, 6.195	57.6652	0.0002	**	1, 6.8801	35.772	0.00059	***
Block§	1	15.683	<.0001	***	1	15.683	<.0001	***
CFR-NIL family line§	1	0.00	1		1	0.00	1	

†Test statistic is *F* for fixed effects and χ^2 for random effects

‡Refers to initial allele frequency category: Low = 34% *MM*, Med = 50% *MM*, High = 66% *MM*

§Random effects; significance tested via LRT

Supplementary Table 2. Effect of herbivory on two reproductive fitness components: probability of reproduction (**A**) and total reproductive output (number of fruits x average fruit set, given reproduction) (**B**). Model A assess the effect of herbivory on reproduction across 8 common garden environments. Model B focuses on one common garden environment (SCH-2016).

Model term	β_{damage}	DF	χ^2	*P*	
A) Probability of reproduction (N = 3,094)					
Environment		7	157.1201	<.0001	***
Herbivore damage	-0.034	1	6.1178	0.01339	*
Damage×Env		7	33.2727	<.0001	***
Block[§]		1	138.37	<.0001	***
B) log(Total reproductive output, given reproduction) (N = 848)					
Herbivore damage	-0.007	1	5.5318	0.01867	*
Block[§]		1	32.327	<.0001	***

[§]Random effect; significance tested via LRT

Supplementary Table 3. Effects of *BCMA1/3* on survival across environments in manipulative field arrays in six environments (**A**) and permanent field transplants in nine environments (**B**).

Model term	Wald test				Parametric bootstrap			
	DF	χ^2	Pr(>ChiSq)		DF	χ^2	Pr(>ChiSq)	
A) Arrays (N = 5,880)								
BCMA1/3	1	5.2690	0.02171	*	8	31.804	0.000999	**
Environment	5	89.2772	$<2.2 \times 10^{-16}$	***	10	81.558	0.00158	**
BCM1/3×Env	5	26.6144	6.8×10^{-5}	***	5	27.839	0.0010	**
Frequency[†]	2	1.7201	0.4231		4	1.8907	0.7942	
BCMA1/3×Frequency[†]	2	0.5318	0.7665		2	0.5189	0.7782	
Block[§]	1	265.42	$<2.2 \times 10^{-16}$	***	1	265.42	$<2.2 \times 10^{-16}$	***
CFR-NIL family line [§]	1	63.704	1.45×10^{-15}	***	1	63.704	1.45×10^{-15}	***
B) Transplants (N = 6,860)								
BCMA1/3	1	1.6359	0.20089		9	61.813	0.0010	**
Environment	8	198.1484	$<2.2\times10^{-16}$	***	16	94.55	0.000999	**
BCMA×Env	8	61.4704	2.397×10^{-10}	***	8	61.769	0.0010	**
Block[§]	1	715.59	$<2.2 \times 10^{-16}$	***	1	715.59	$<2.2 \times 10^{-16}$	***
CFR-NIL family line [§]	1	27.033	2.0×10^{-7}	***	1	27.033	2.0×10^{-7}	***

[†]Refers to initial allele frequency category: Low = 34% *MM*, Med = 50% *MM*, High = 66% *MM*

[§]Random effects; significance tested via LRT

Supplementary Table 4. Effect of herbivory in 2016 on survival to 2017 in the Schofield (SCH) common garden (N = 1,219).

Model term	β_{damage}	DF	χ^2	*P*	
Herbivore damage	-0.014	1	1.2975	0.2547	
Block[§]		1	52.721	<.0001	***

[§]Random effect

Supplementary Table 5. Effects of viability selection on final *BCMA1/3* genotype frequencies in temporary arrays, including all field arrays (**A**), or excluding array #34, an outlier with extremely high viability selection (proportion mortality = 0.72) (**B**).

Model term	DF	Sum Sq	*F*	Pr(>*F*)	
A) All arrays (N = 60)					
Proportion mortality (β=0.231)	1	0.01824	29.1252	<.0001	***
Environment	5	0.00414	1.3221	0.2704	
Frequency†	2	0.85515	682.8889	<.0001	***
Frequency† × prop. mortality	2	0.00529	4.2228	0.0203	*
B) Outlier excluded (N = 59)					
Proportion mortality (β=0.146)	1	0.00630	21.8870	<.0001	***
Environment	5	0.00176	1.2208	0.3139	
Frequency†	2	0.88294	1532.878	<.0001	***
Frequency† × prop. mortality	2	0.00036	0.6319	0.5359	

†Refers to initial allele frequency category:
Low = 34% *MM*, Med = 50% *MM*, High = 66% *MM*

Supplementary Table 6. Effects of *BCMA* on morphological responses to drought. Each table row represents a separate model and columns are model effects. Bold values denote $P < 0.05$.

Response variable (N)	Fixed effect (df)								Random effect (df)			
	Initial height (1)		*BCMA* (1)		Drought (1)		*BCMA*×Drought (1)		Block (1)		CFR-NIL family (1)	
	χ^2	*P*	χ^2	*P*	χ^2	*P*	χ^2	*P*	χ^2	*P*	χ^2	*P*
Final height (954)	282.03	**2.2×10^{-16}**	0.79	0.3735	9.13	**0.0025**	27.32	**1.73×10^{-7}**	91.87	**2.2×10^{-16}**	23.62	**1.18×10^{-6}**
Total leaves (958)	413.63	**2.2×10^{-16}**	0.94	0.3330	4.02	**0.0451**	8.52	**0.0035**	17.41	**3.01×10^{-5}**	0.91	0.3390
Estimated LMA (568)	7.38	**0.0066**	0.46	0.4965	3.01	0.0825	1.51	0.2197	3.19	0.0739	0.65	0.4219
Leaf width (951)	165.25	**2.2×10^{-16}**	0.61	0.4329	6.13	**0.0133**	25.44	**4.55×10^{-7}**	84.07	**2.2×10^{-16}**	33.56	**6.9×10^{-9}**
Growth rate (954)	215.28	**2.2×10^{-16}**	0.79	0.3735	9.13	**0.0025**	27.32	**1.73×10^{-7}**	91.87	**2.2×10^{-16}**	23.62	**1.18×10^{-6}**
Green leaves (959)	50.99	**9.3×10^{-13}**	10.36	**0.0013**	4.74	**0.0294**	22.79	**1.81×10^{-6}**	10.26	**0.0014**	3.87	**0.0491**
Leaf water content (569)	114.79	**2.0×10^{-16}**	0.93	0.3360	95.97	**2.0×10^{-16}**	3.14	0.0764	144.66	**2.2×10^{-16}**	0	1

Supplementary Table 7. Effects of genotype and morphology on water use under drought. Models A-C capture net effects of each trait on water use; model D accounts for covariance among traits. LMA = leaf mass per area.

Model (N)	Model effect	DF	χ^2	*P*	
A	*BCMA1/3*	1	0.0943	0.7588	
(486)	Initial height	1	52.9137	3.49×10^{-13}	***
	Final height	1	12.8290	0.0003	***
	BCMA1/3×final height	1	0.5051	0.4773	
	Block[§]	1	81.558	$<2.2\times10^{-16}$	***
	CFR-NIL family line[§]	1	12.934	0.0003	**
B	*BCMA1/3*	1	0.4522	0.5013	
(487)	Total leaves	1	44.0913	3.13×10^{-11}	***
	BCMA1/3×Total leaves	1	0.0190	0.8902	
	Block[§]	1	71.564	$<2.2\times10^{-16}$	***
	CFR-NIL family line[§]	1	29.934	4.47×10^{-8}	***
C	*BCMA1/3*	1	0.0794	0.7781	
(477)	Estimated LMA	1	22.4542	2.15×10^{-6}	***
	BCMA1/3×LMA	1	1.4383	0.2304	
	Block[§]	1	77.804	$<2.2\times10^{-16}$	***
	CFR-NIL family line[§]	1	35.192	2.99×10^{-9}	***
D	*BCMA1/3*	1	2.8861	0.08935	.
(478)	Initial height	1	25.9175	3.56×10^{-7}	***
	Final height	1	19.1444	1.21×10^{-5}	***
	Total leaves	1	1.0186	0.3128	
	Estimated LMA	1	3.8965	0.0484	*
	Block[§]	1	79.661	$<2.2\times10^{-16}$	***
	CFR-NIL family line[§]	1	12.696	0.0004	**

[§]Random effect

Supplementary Table 8. Effect of BC-ratio on leaf water content under drought, controlling for population structure in three ways: with discrete genetic groups (**A**), with principal components 1-5 of genome-wide variation in the full panel of accessions (**B**), and with principal components 1-5 of genome-wide variation in COL+UTA genotypes (**C**), which have high genetic variation and low LD around *BCMA3*.

Model (N)	Model term	$\beta_{\text{BC-ratio}}$	Sum Sq	DF	F	Pr(>F)	
A (237)	BC-ratio	-2.63×10^{-5}	0.0002	1	8.1709	0.004646	***
	Genetic group		0.0001	4	1.2381	0.295475	
B (255)	BC-ratio	-2.18×10^{-5}	0.0001	1	6.7133	0.01014	*
	Genomic PC1		0.0000	1	0.0399	0.84176	
	Genomic PC2		0.0000	1	0.5218	0.47074	
	Genomic PC3		0.0000	1	0.1606	0.68898	
	Genomic PC4		0.0000	1	0.1606	0.68898	
	Genomic PC5		0.0000	1	0.8216	0.36559	
C (110)	BC-ratio	-2.46×10^{-5}	0.0001	1	3.7000	0.05717	.
	Genomic PC1		0.0000	1	0.7376	0.39242	
	Genomic PC2		0.0000	1	0.0398	0.84222	
	Genomic PC3		0.0001	1	3.4751	0.06515	.
	Genomic PC4		0.0000	1	0.4786	0.49061	
	Genomic PC5		0.0000	1	1.4276	0.23490	

Supplementary Table 9. Effects of geography and climate of origin on genetic mean BC-ratio across a broad panel of genotypes, controlling for population structure in three ways: with discrete genetic groups (**A**), with principal components 1-5 of genome-wide variation in the full panel of accessions (**B**), and with principal components 1-5 of genome-wide variation in COL+UTA genotypes (**C**), which have high genetic variation and low LD around *BCMA3*.

Model (N)	Model Effect	β	DF	Sum Sq.	F	Pr > F	
A (283)	Genetic group		4	11399	2.9778	0.019735	*
	Latitude	-3.20	1	1235	1.2901	0.257037	
	Longitude	3.88	1	2864	2.9925	0.084796	
	Elevation	-0.06	1	5438	5.6823	0.017829	*
	Climate PC1	6.04	1	14456	15.1060	0.000128	***
	Climate PC2	0.43	1	65	0.0675	0.795247	
	Climate PC3	-2.20	1	1131	1.1814	0.278047	
	Climate PC4	-4.37	1	3025	3.1613	0.076528	.
	Climate PC5	-1.38	1	273	0.2850	0.593879	
B (301)	Latitude	-0.02	1	0	0.0001	0.992262	
	Longitude	0.76	1	201	0.2054	0.650762	
	Elevation	-0.05	1	5322	5.4269	0.020523	*
	Genomic PC1	-68.89	1	891	0.9082	0.341403	
	Genomic PC2	-9.51	1	28	0.0286	0.865896	
	Genomic PC3	-36.26	1	415	0.4236	0.515689	
	Genomic PC4	-75.95	1	2601	2.6522	0.104502	
	Genomic PC5	-32.33	1	736	0.7500	0.387192	
	Climate PC1	5.41	1	13227	13.4883	0.000286	***
	Climate PC2	1.97	1	1310	1.3356	0.248768	
	Climate PC3	-3.90	1	4723	4.8164	0.028992	*
	Climate PC4	-3.25	1	1814	1.8502	0.174831	
	Climate PC5	-1.87	1	462	0.4709	0.493110	
C (132)	Latitude	-6.81	1	2161	1.8978	0.170930	
	Longitude	4.05	1	1221	1.0720	0.302620	
	Elevation	-0.10	1	6513	5.7204	0.018349	*
	Genomic PC1	111.68	1	2205	1.9370	0.166613	
	Genomic PC2	84.93	1	886	0.7785	0.379386	
	Genomic PC3	-75.05	1	3131	2.7500	0.099913	.
	Genomic PC4	-42.80	1	982	0.8629	0.354833	
	Genomic PC5	66.09	1	2244	1.9711	0.162960	
	Climate PC1	10.06	1	8042	7.0631	0.008959	**
	Climate PC2	-0.22	1	5	0.0044	0.947040	
	Climate PC3	-6.99	1	3269	2.8708	0.092840	.
	Climate PC4	-10.11	1	4399	3.8634	0.051700	.
	Climate PC5	-4.44	1	700	0.6146	0.434617	

Supplementary Table 10. Summary of first five principal components for climate variation at the location of origin of 283 genotypes of *B. stricta*. Bold values are highly correlated ($|r| > 0.70$) with climate PCA axis 1, which significantly predicts BC-ratio.

Climate Variable		Climate loading onto axis (cumulative % climate variation explained)				
BioClim	**Full name**	**PC1 (34.13)**	**PC2 (59.96)**	**PC3 (74.28)**	**PC4 (84.46)**	**PC5 (91.10)**
bio1_12	Mean annual temperature	-0.4753	0.7486	0.3496	0.0835	0.1623
bio2_12	Mean diurnal range (Mean of monthly (max temp – min temp)	-0.4727	-0.5377	-0.4206	0.4082	0.1426
bio3_12	Isothermality ((BIO2/BIO7)*100)	-0.0783	-0.0466	-0.8218	0.1303	-0.1152
bio4_12	Temperature seasonality (standard deviation*100)	-0.4451	-0.5547	0.5123	0.2518	0.3288
bio5_12	Max temperature of warmest month	**-0.7726**	0.2887	0.2794	0.3561	0.1859
bio6_12	Min temperature of coldest month	-0.0136	0.9360	0.1678	-0.1864	-0.1588
bio7_12	Temperature annual range (BIO5-BIO6)	-0.5540	-0.6476	0.0508	0.4322	0.2820
bio8_12	Mean temperature of wettest quarter	-0.5892	0.0137	-0.0765	-0.5478	0.3261
bio9_12	Mean temperature of driest quarter	0.4699	0.1821	0.4034	0.6091	-0.2008
bio10_12	Mean temperature of warmest quarter	-0.5753	0.5276	0.5442	0.1245	0.2400
bio11_12	Mean temperature of coldest quarter	-0.1440	0.9322	0.1274	-0.1103	-0.0569
bio12_12	Annual precipitation	**0.9388**	0.0901	0.1163	0.0980	0.2451
bio13_12	Precipitation of wettest month	**0.7497**	0.4185	-0.2749	0.1253	0.3900
bio14_12	Precipitation of driest month	**0.7274**	-0.3984	0.4770	-0.0829	-0.0345
bio15_12	Precipitation seasonality (coefficient of variation)	-0.0932	0.5906	-0.6170	0.1526	0.3342
bio16_12	Precipitation of wettest quarter	**0.7834**	0.3999	-0.1860	0.1968	0.3680
bio17_12	Precipitation of driest quarter	**0.7639**	-0.4066	0.3925	-0.1498	0.0190
bio18_12	Precipitation of warmest quarter	0.3803	-0.3239	0.0856	-0.5638	0.5347
bio19_12	Precipitation of coldest quarter	**0.8478**	0.1833	-0.0238	0.4446	0.0283

Supplementary Table 11. Association of climate predictors with BC-ratio, controlling for population structure in three ways: with discrete genetic groups (**A**), with principal components 1-5 of genome-wide variation in the full panel of accessions (**B**), and with principal components 1-5 of genome-wide variation in COL+UTA genotypes (**C**), which have high genetic variation and low LD around *BCMA3*. Bold values indicate significant effects of climate on BC-ratio.

Climatic variable	Model approach (N)	Model effect	$\beta_{climate}$	Sum Sq	df	*F*	*P*	
							Linear model	Permutation test
bio5 (max temp. in warmest mo.)	**A** (283)	Climate	-0.12	1447	1	1.40	0.23696	0.2383
		Genetic group		58590	4	14.22	1.45×10^{-10}	<0.0001
	B (303)	Climate	-0.03	109	1	0.10	0.75686	0.75910
		Genomic PC1		8341	1	7.34	0.00714	0.00680
		Genomic PC2		4360	1	3.84	0.05108	0.04990
		Genomic PC3		13103	1	11.53	0.00078	0.00070
		Genomic PC4		45	1	0.04	0.84198	0.84090
		Genomic PC5		1847	1	1.62	0.20343	0.19740
	C (132)	Climate	-0.21	1446	1	1.07	0.30332	0.30380
		Genomic PC1		8208	1	6.07	0.01515	0.01760
		Genomic PC2		2504	1	1.85	0.17618	0.18050
		Genomic PC3		7858	1	5.81	0.01742	0.01510
		Genomic PC4		3599	1	2.66	0.10545	0.10200
		Genomic PC5		49	1	0.04	0.84950	0.84610
bio12 (annual precip.)	**A** (283)	Climate	0.07	12555	1	12.68	**0.0004**	**0.0008**
		Genetic group		65541	4	16.54	3.60×10^{-12}	<0.0001
	B (303)	Climate	0.07	10257	1	9.31	**0.00025**	**0.00260**
		Genomic PC1		9808	1	8.90	0.00309	0.00270
		Genomic PC2		9659	1	8.75	0.00334	0.00310
		Genomic PC3		17319	1	15.71	9.25×10^{-5}	0.00020
		Genomic PC4		471	1	0.43	0.51364	0.51080
		Genomic PC5		1714	1	1.56	0.21333	0.21090
	C (132)	Climate	0.14	10826	1	8.47	**0.00428**	**0.00480**
		Genomic PC1		8137	1	6.37	0.01288	0.01270
		Genomic PC2		548	1	0.43	0.51374	0.52120
		Genomic PC3		2473	1	1.93	0.16673	0.16640
		Genomic PC4		361	1	0.28	0.59608	0.59960
		Genomic PC5		664	1	0.52	0.47253	0.46960
bio13 (precip. in wettest mo.)	**A** (283)	Climate	0.51	10511	1	10.54	**0.0013**	**0.0016**
		Genetic group		46721	4	11.71	8.47×10^{-9}	<0.0001
	B (303)	Climate	0.77	24271	1	23.01	**2.56×10^{-6}**	**<0.0001**
		Genomic PC1		9302	1	8.82	0.00323	0.00320
		Genomic PC2		10024	1	9.50	0.00225	0.00190
		Genomic PC3		9905	1	9.39	0.00238	0.00250
		Genomic PC4		1779	1	1.69	0.19514	0.19770
		Genomic PC5		1946	1	1.84	0.17544	0.17890
	C (132)	Climate	1.28	17118	1	13.94	**0.00029**	**0.00020**
		Genomic PC1		5053	1	4.12	0.04462	0.04720
		Genomic PC2		3644	1	2.97	0.08742	0.09110
		Genomic PC3		3228	1	2.63	0.10742	0.10260
		Genomic PC4		200	1	0.16	0.68705	0.68170
		Genomic PC5		681	1	0.55	0.45791	0.45470
bio14 (precip. in driest mo.)	**A** (238)	Climate	0.70	4346	1	4.26	**0.0399**	**0.0382**
		Genetic group		60517	4	14.83	5.39×10^{-11}	<0.0001
	B (303)	Climate	0.05	28	1	0.02	0.87473	0.87240
		Genomic PC1		8267	1	7.27	0.00740	0.00780

		Genomic PC2		4122	1	3.63	0.05785	0.06360
		Genomic PC3		11678	1	10.27	0.00150	0.00200
		Genomic PC4		33	1	0.03	0.86470	0.86690
		Genomic PC5		1756	1	1.54	0.21491	0.21450
	C (132)	Climate	1.00	1894	1	1.40	0.23845	0.24260
		Genomic PC1		9157	1	6.78	0.01031	0.01100
		Genomic PC2		61	1	0.05	0.83220	0.82980
		Genomic PC3		9614	1	7.12	0.00862	0.00700
		Genomic PC4		3329	1	2.47	0.11879	0.12080
		Genomic PC5		26	1	0.02	0.88920	0.89000
bio16	**A** (283)	Climate	0.19	11407	1	11.47	**0.0008**	**0.0010**
(precip. in wettest quarter)		Genetic group		50361	4	12.66	1.78×10^{-9}	<0.0001
	B (303)	Climate	0.27	24288	1	23.03	$\mathbf{2.54\times10^{-6}}$	**<0.0001**
		Genomic PC1		9794	1	9.28	0.00252	0.00270
		Genomic PC2		9965	1	9.45	0.00231	0.00210
		Genomic PC3		13645	1	12.94	0.00038	0.00050
		Genomic PC4		1982	1	1.88	0.17148	0.16860
		Genomic PC5		2004	1	1.90	0.16909	0.16230
	C (132)	Climate	0.48	18711	1	15.40	**0.00014**	**0.00010**
		Genomic PC1		7990	1	6.58	0.01152	0.01310
		Genomic PC2		1116	1	0.92	0.33973	0.34740
		Genomic PC3		3963	1	3.26	0.07331	0.06770
		Genomic PC4		8	1	0.01	0.93502	0.93570
		Genomic PC5		502	1	0.41	0.52162	0.52810
bio17	**A** (283)	Climate	0.25	5320	1	5.23	**0.0229**	**0.0223**
(precip. in driest quarter)		Genetic group		61719	4	15.18	3.10×10^{-11}	<0.0001
	B (303)	Climate	0.01	8	1	0.01	0.93315	0.93270
		Genomic PC1		8240	1	7.25	0.00750	0.00810
		Genomic PC2		3955	1	3.48	0.06316	0.06530
		Genomic PC3		12131	1	10.67	0.00122	0.00140
		Genomic PC4		35	1	0.03	0.86013	0.86610
		Genomic PC5		1783	1	1.57	0.21144	0.21090
	C (132)	Climate	0.20	897	1	0.66	0.41779	0.42300
		Genomic PC1		7955	1	5.86	0.01693	0.01660
		Genomic PC2		1095	1	0.81	0.37088	0.36750
		Genomic PC3		7966	1	5.87	0.01685	0.01710
		Genomic PC4		2578	1	1.90	0.17061	0.16530
		Genomic PC5		67	1	0.05	0.82426	0.82370
bio19	**A** (283)	Climate	0.08	3832	1	3.75	0.0538	0.0537
(precip. in coldest quarter)		Genetic group		56035	4	13.71	3.26×10^{-10}	<0.0001
	B (303)	Climate	0.12	8326	1	7.51	**0.00651**	**0.00710**
		Genomic PC1		8531	1	7.69	0.00589	0.00530
		Genomic PC2		7100	1	6.40	0.01191	0.01140
		Genomic PC3		16684	1	15.05	0.00013	0.00020
		Genomic PC4		641	1	0.58	0.44764	0.45560
		Genomic PC5		1786	1	1.61	0.20542	0.21440
	C (132)	Climate	0.12	1012	1	0.75	0.38941	0.39440
		Genomic PC1		6659	1	4.91	0.02854	0.02990
		Genomic PC2		1058	1	0.78	0.37884	0.38410
		Genomic PC3		8736	1	6.44	0.01239	0.00970
		Genomic PC4		1264	1	0.93	0.33624	0.34280
		Genomic PC5		384	1	0.28	0.59582	0.58590

30

Supplementary Table 12. Effects of *BCMA3* structural variation (**A**) and BCMA3 enzyme amino acid variation (**B**-**C**) on BC-ratio.

Model (N)	Model effect	Sum sq.	df	*F*	*P*	
A (82)	Genetic group	9763	4	3.4483	0.01215	*
	Premature stop	4823	1	6.8141	0.01091	*
	8 bp deletion	151	1	0.2139	0.64504	
B (69)	Genetic group	3368	4	1.0331	0.3974	
	Concatenated AA phenotype	2070	2	1.2698	0.2881	
C (69)	Genetic group	3368	4	1.0331	0.3974	
	AA148	1642	1	2.0145	0.1608	
	AA268	360	1	0.4422	0.5085	

Note: Sample sizes reflect the subset of genotypes with Sanger data, group assignments (Wang et al. 2019), and BC-ratio phenotype data. Models **B** and **C** are further subsetted to focus on genotypes with full-length *BCMA3* exons.

Supplementary Table 13. List of known aliphatic glucosinolates (GS) in *B. stricta* and internal standard in HPLC, with retention times used to call peaks. Chemical names and amino acid (AA) precursors *sensu* Windsor et al. (2005).

Abbrev.	Full name*	AA precursor	Retention time in HPLC (min)
2OH1ME	ds-hydroxymethylethyl-GS	Valine	1.16
5MSOP	ds-5-methylsulfinylpentyl-GS	Methionine	2.47
Sinalbin**	ds-4-hydroxybenzyl-GS	Tyrosine	2.81
6MSOH	ds-6-methylsulfinylhexyl-GS	Methionine	3.52
1MP	ds-1-methylpropyl-GS	Isoleucine	3.96
1ME	ds-1-methylethyl-GS	Valine	2.70

*ds = desulfo- (all sulfate groups removed by treatment with sulfatase during GS extraction)

**internal standard used in HPLC runs; not produced in *B. stricta*

Supplementary Table 14. Summary of *BCMA1/3* CFR-NIL transplants across years and sites.

State	Garden Site	Shorthand	Census Year	Transplant cohort	N planted	N obs. herbivory
ID	Alder	ALD	2013	Spring 2013	720	384
			2014	Fall 2013	360	302
			2015	Fall 2014	855	334
	Mahogany	MAH	2014	Fall 2013	540	252
			2015	Fall 2014	570	348
	Silver	SIL	2014	Fall 2013	450	265
			2015	Fall 2014	665	406
CO	Gothic	GTH	2016	Fall 2015	1,350	293
	Schofield	SCH	2016	Fall 2015	1,350	1,090
Total:					6,860	3,674

Supplementary Table 15. Comparisons between *Boechera stricta* LTM (MT) genome from version_1.2 (Lee *et al.* 2017) and version_2 assemblies.

Attribute	version_1.2	version_2
Assembly size (Mb)	189.35	189.86
Amount of nucleotide N (Mb)	24.51	0
Scaffold number*	1990	34
Scaffold N50 (Mb)	2.19	13.80
Largest scaffold (Mb)	8.34	22.91
BUSCO score (%)	96.40	98.50
Scaffolds on chromosome	208	27
Size on chromosome (Mb)	183.72	188.87

*For version_1.2, scaffolds refer to the group of contigs connected together by mate-pair Illumina sequences. For v2, scaffolds refer to the contigs directly assembled from Nanopore reads.

Supplementary Table 16. Accessions retained in Sanger sequencing analyses, by genetic group.

Group	N accessions	
	Full panel	**Sanger sequencing**
COL	157	36
NOR	105	18
UTA	126	18
WES	79	22
Admixed	17	6
Unassigned	0	10
Totals	484	110

Supplementary Table 17. Primers used to amplify and sequence *BCMA3*.

Primer name	Direction	Use	Sequence
oCO-188	R	Amplification	TTTATTGCGGATTCACCTCA
oCO-242	F	Amplification	TTTCATCCAAAACAAAGTTATGC
oCO-108	R	Sequencing	GTTTCTCTGCAACAAGCTTTTAAG
oCO-232	F	Sequencing	AACGTGATCGGCTTAGTACCTACC
oCO-233	F	Sequencing	CGCAGTGACCATGAGAATGT
oCO-234	F	Sequencing	AATCCGGCAAATAACATGGA
oCO-235	F	Sequencing	CCAACCACGTTTATTCGTCA
oCO-261	R	Sequencing	TCCTTTTGGTCGGAATTCAA

Supplementary Table 18. Contingency table showing the co-occurrence of putative functional amino acid substitutions and structural genetic variation in 110 *BCMA3* alleles. Blue column indicates residues observed in the SAD12 accession; red column indicates residues observed in the LTM accession. Asterisks (*) indicate premature stop codons upstream of the residues of interest.

		***BCMA3* amino acid residues (positions 148 and 268)**			
		LV	**VV**	**VM**	******
***BCMA3* structural variant**	**Complete exons + no deletion**	18	51	18	0
	Premature stop + no deletion	3	0	0	0
	Premature stop + 8bp deletion	0	0	0	20

Supplementary methods and results

Characterizing GS variation

Boechera stricta produces glucosinolates (GS) from a variety of amino acid precursors (Windsor et al. 2005). Of particular interest, this species synthesizes GS from several branched-chain (BC) amino acids (Val, Ile, Leu; Schranz et al. 2009, Prasad et al. 2012) in addition to the ancestral methionine biosynthetic activity displayed in *Arabidopsis* and other close relatives (Windsor et al. 2005). Met- and BC-derived GS are aliphatic GS, meaning that they are derived from amino acids with aliphatic side chains. Conversely, other species in the Brassicaceae, including some *Boechera*, also produce indolic (Trp-derived) and benzenic (Phe- or Tyr-derived) GS (Windsor et al. 2005). Here, we focus on aliphatic compounds commonly produced in *B. stricta* leaves (**Supplementary Table 13**), as have previously been well characterized (Schranz et al. 2009, Prasad et al. 2012).

Aliphatic glucosinolate production occurs via two main stages: (1) GS core biosynthesis and (2) side chain modification. Stage 1 controls the amino acid precursors that are utilized in GS biosynthesis, their elongation (when it occurs), and the conversion into the "glucosinolate core". Stage 2 controls functional modification of amino acid side chains ("R-groups") via oxidation, hydroxylation, and/or esterification. Together, these processes result in >100 known specific GS compounds produced by presence/absence of and allelic variation in biosynthetic genes regulating different steps in the pathway (Windsor et al. 2005, Sønderby et al. 2010). *Arabidopsis CYP79F1/2* genes regulate the first step in core synthesis, encoding proteins that convert elongated Met derivatives to aldoximes (Sønderby et al. 2010). The orthologous *BCMA2* and *BCMA1/3* genes in *Boechera stricta* encode CYP79 proteins with broader amino acid substrate affinity converting Val, Ile, and Met (plus elongated derivatives) to their corresponding aldoximes. The sequence and relative activity of the BCMA2 vs. BCMA1/3 proteins determine the balance between branched chain (Val, Ile)- and Met-derived GS synthesized by the plant (Prasad et al. 2012).

We characterized the identity and quantity of different GS produced in all accessions using high-performance liquid chromatography (HPLC), as described below.

Plant care

We germinated seedlings of each accession in petri dishes, and then transplanted germinants into potting soil (80% Fafard 4P Mix, Conrad Fafard, Agawam, MA; 20% Sunshine MVP, SunGro Horticulture, Vancouver, BC) in 4" cone-tainers (Stuewe & Sons Inc., Tangent, OR). We grew 20 replicates per accession in a randomized, complete-block design under controlled greenhouse conditions (18-21° C day / 13-16° C night; 16 h day length; watering to saturation daily; fertilization at 300 ppm N weekly) in Durham, NC.

GS extraction

When transplants reached 4 weeks in age, we harvested a single fresh leaf (~30 mg) per individual, flash-froze the tissue in liquid N_2, and then freeze-dried the samples. We weighed each freeze-dried leaf and ground the tissue with two 2.38 mm steel ball bearings (V and P Scientific, San Diego, CA) in each 1.4 mL tube (COMO RACK™, Micronic, Aston, PA) using a

Geno/Grinder® automated tissue homogenizer and cell lyser (Spex® Sample Prep, Metuchen, NJ, USA)**.** We extracted desulfoglucosinolates from the ground, freeze-dried tissue according to Burow et al. (2006), with modifications for high-throughput analyses.

We extracted GS in 1 mL 80% methanol (v:v) containing 50 µM sinalbin (as an internal standard) on a shaker at 150 rpm at room temperature for 30 min. We clarified extracted mixtures by centrifuging samples at 3,200 g for 10 min and adding supernatant (700 µl) to a pre-equilibrated (80% methanol; v:v) DEAE Sephadex ion exchange column (28mg per sample, Sigma-Aldrich). We washed the column once with 0.5 mL 80% methanol (v:v), two times with 1 mL of water, and once with 0.5 mL 0.02 M MES buffer, pH 5.2. After washing, we added 30 µl of sulfatase from *Helix pomatia* (280 units/mL) solution (Sigma-Aldrich) on top of each column, and incubated samples at room temperature for 16 h. We eluted desulfo-glucosinolates from the columns in 0.5 mL of sterile deionized water.

HPLC

We determined the identity and quantity of different GS (**Supplementary Table 13**) in each plant sample using HPLC with an Agilent 1100 system equipped with a 96-well-plate autosampler and diode-array detector. We separated GS from extracted mixtures on a C-18 column (Zorbax Eclipse XDB-C18, 4.6 x 50 mm, 1.8 µm) using a water ("solvent A") and acetonitrile ("solvent B") solvent gradient at a flow rate of 1.1 mL min^{-1} at a temperature of 25° C. The solvent gradient during each 7.5 min run progressed as follows: 2% to 14% (v/v) B (0-4 min); 14% to 100% (v/v) B (4-4.1 min); 100% (v/v) B (4.1-5 min); 100% to 2% (v/v) B (5-5.1 min); and 2% (v/v) B (5.1-7.5 min). We monitored eluents by diode array detection between 190 and 360 nm at 2 nm intervals. We identified the GS of specific eluents by retention time (**Supplementary Table 13**) and by comparison of UV absorption spectra at 229 nm to those of isolated standard compounds. Furthermore, we confirmed the identity of ds-GS using liquid chromatography - electrospray mass spectrometry (LC-ESI-MS) on a Bruker Esquire 6000 ion trap mass spectrometer (Bruker Daltonics, Bremen, Germany). We report results as µmol (g dry weight)$^{-1}$ calculated from the peak areas at 229 nm relative to the peak area of the internal standard using the relative response factors 2.0 for all aliphatic glucosinolates (Burow et al. 2006).

Genetic means of GS phenotypes

From the full GS profiles for each individual, we calculated BC-ratio as follows:

$$BC\text{-}ratio = \frac{BC\text{-}GS}{Total\ GS} = \frac{1ME + 2OH1ME + 1MP}{1ME + 2OH1ME + 1MP + 6MSOH + 5MSOP}$$

We estimated the least-squares mean value and standard error of BC-ratio per accession by REML mixed model in JMP Pro v. 13, regressing BC-ratio onto the random effects of accession ID and complete statistical block within the greenhouse. We visualized variation in these genetic mean values in response to the location of origin for each accession using the 'ggmap' package v. 3.0.0 in R (Kahle and Wickham 2013).

Generation of CFR-NILs

DNA extraction, primers, and PCR methods for all crossing and genotyping are described in the Supplementary Online Information of Prasad et al (2012). Previously we identified 205 F5

individuals derived from crosses between the LTM and SAD12 parental accessions (referred to as RP072 and RP067, respectively, in Wang et al. 2019) that were recombinant in the *BCMA1/3* region; selfed these plants; and scored the F6 progeny for 13 tightly-linked polymorphic markers to identify homozygotes with recombination near *BCMA1/3* (Prasad et al. 2012) (**Extended Data Figure 6**). We chose two F6s showing recombinants close to *BCMA1/3* (subsequently verified by GBS), which we refer to as closest flanking recombinants (CFRs). We crossed the two CFR genotypes to generate an F1 progeny ("KAS-38"), and selfed this to generate F2s. We identified multiple independent homozygous *BB* and *MM* F2 genotypes, which we call "family lines" (**Extended Data Figure 6**), using PCR marker BSTES0008 (Prasad et al. 2012), and verified the expected GS profiles of *BB* and *MM* homozygotes using HPLC. By retaining multiple independent family lines within the homozygous *BB* and *MM* genotypes, we controlled for possible confounding effects of variable loci elsewhere in the genome. We bulked seeds from each family line via selfing, and used F3 or later selfed progenies in all experiments.

Common garden experiments

Plant care and transplanting

We grew replicate individuals of each homozygous CFR-NIL family (full sibs derived from self-pollination) in spatially randomized, complete blocks at Duke University. We grew germinants for 1-2 months under controlled greenhouse conditions (above), and then shipped established rosettes overnight to field locations. In the field, we transplanted individuals in a randomized complete block design at 10 cm intervals into the matrix of native vegetation in common gardens. Gardens were fenced to exclude megaherbivores, but insects and small vertebrates could freely browse experimental plants. Garden cohorts contained 360–1,350 individuals each (**Supplementary Table 14**) and each contained at least four replicate CFR-NIL families per genotype to account for possible effects of unlinked loci outside of the *BCMA1/3* region.

Field measurements

Because mortality in the field is high, we collected data on most transplants in a single summer following the planting of each cohort, during which sample sizes were largest. For all experimental plants (transplants and arrays), we censused each plant in mid to late growing season to score survival (0 or 1) and estimated total percent tissue lost to herbivores as described in Wagner & Mitchell-Olds (2018).

B. stricta requires cold-cueing (vernalization) in order to flower, so we could measure reproductive output in cohorts of transplants which were planted in the autumn prior to the census year. This included all common garden environments except for ALD-2013 in Idaho **(Supplementary Table 14).** We scored all individuals for reproduction (0/1) at the end of the growing season as an estimate of reproductive fitness. In one environment where survival and reproduction were high (SCH-2016), we also measured silique length, and estimated total reproductive output by multiplying silique number by mean silique length, since total silique length is a reliable proxy for total seed number (Wadgymar et al. 2017).

Natural selection for herbivore resistance

For experimental individuals in environments that allowed reproduction (N = 3,094), we tested for natural selection on herbivore defense by regressing reproductive success (0/1) onto fixed effects of herbivore damage, environment, and the damage×environment interaction and a random effect of block using a generalized linear mixed effects regression with a binomial distribution and logit link function (**Supplementary Table 2A**). Among reproductive individuals in the SCH-2016 environment, we modeled log-transformed total reproductive output in response to the fixed effect of herbivore damage and a random effect of block using a linear mixed effects model (**Supplementary Table 2B**).

We also tested for the effects of herbivore damage on survival in a subset of transplants in one environment (SCH-2016 in Colorado; N = 1,219) which we monitored for multiple years. Specifically, we regressed survival in 2017 upon herbivore damage in 2016 using a generalized linear mixed effects model ('glmer' function) with a binomial distribution, accounting for block within the garden as a random effect (**Supplementary Table 4**).

For all of these analyses, we fit models using the 'lme4' package v. 1.1-23 (Bates et al. 2015). We tested the significance of fixed effects using Type III Wald chi-square tests with the 'Anova' function in the 'car' package v. 3.0-9 (Fox & Weisberg 2019). We tested the significance of random effects using likelihood ratio tests, comparing the full model to a nested reduced model containing a single-term deletion of the random effect. We performed all analyses in R v. 4.0.2 (R Core Team 2020).

Variation in herbivore resistance across environments

To assess the role of heterogeneous selection on the evolution of GS diversity in *B. stricta*, we tested for variation in the effects of *BCMA1/3* alleles on herbivore resistance, which contributes to reproductive fitness (**Figure 2B; Supplementary Table 2**; Prasad et al. 2012). Specifically, we used REML mixed-effects models in JMP Pro v. 14.3.0 to test for *BCMA* × environment effects on herbivore damage, including random effects of statistical block and CFR-NIL line nested within genotype. Because herbivore damage could only be measured on plants that survived to the census date, our models retained 3,674 observations of herbivory from 6,860 transplants (**Supplemental Table 14**).

To validate the outcomes of these tests, we also fit all models using the 'lme4' package (Bates et al. 2015) and tested the significance of fixed effects using the Kenward-Roger method in the 'pbkrtest' package (Halekoh & Højsgaard 2014) in R v. 4.0.2 (R Core Team 2020). Denominator degrees of freedom, test statistic, and P-values for both approaches are reported in **Supplementary Table 1**. Conclusions were qualitatively consistent and quantitatively nearly identical for both approaches. We tested the significance of random effects using likelihood ratio tests comparing the full model to nested, reduced models containing single-term deletions of each random effect.

We extracted least squares means and standard errors of herbivore damage for each genotype in each environment as estimated in the REML models after accounting for other model effects, and plotted this variation using 'ggplot2' v. 3.1.1 in R v. 3.6.0. If our statistical model identified a significant *BCMA1/3* × environment interaction, we used pairwise contrasts in JMP Pro v. 14.3.0 to compare damage levels received by the two *BCMA* homozygotes within each environment.

Variation in survival across environments

Viability selection can have significant impacts on total fitness (Schluter et al. 1991, Crone 2001, Hadfield 2008, Mojica & Kelly 2010, Wadgymar et al. 2017). Therefore, spatial and temporal variation in survival may also influence the maintenance of polymorphisms. We tested for variation in the effects of *BCMA1/3* on survival across environments using a parallel approach to that described above for variation in herbivore resistance. We used a generalized linear mixed effects model ('glmer' function in the 'lme4' package v. 1.1-23) to fit survival in response to fixed effects of *BCMA1/3*, environment, and the *BCMA* × environment interaction, and random effects of garden block and family line. We tested the significance of fixed effects using Type III Wald chi-square tests with the 'Anova' function in the 'car' package v. 3.0-9 (Fox & Weisberg 2019). We performed all analyses in R v. 4.0.2 (R Core Team 2020). We tested the significance of random effects using likelihood ratio tests comparing the full model to nested, reduced models containing single-term deletions of each random effect.

To validate the outcomes of these tests, we also tested the significance of fixed effects using parametric bootstrapping in the 'pbkrtest' package (Halekoh & Højsgaard 2014) in R v. 4.0.2 (R Core Team 2020). Denominator degrees of freedom, test statistic, and P-values for both approaches are reported in **Supplementary Table 3.** Conclusions were qualitatively consistent and quantitatively nearly identical for both approaches.

We calculated least squares mean and standard error values of the probability of survival for each genotype in each environment using the models described above ('emmeans' function using the package 'emmeans' v. 1.3.4), and plotted this variation using 'ggplot2' v. 3.1.1 in R v. 3.6.0. If our statistical models identified a significant *BCMA1/3* × environment interaction, we used pairwise contrasts to compare survival of the two *BCMA1/3* homozygotes within each environment.

Temporary array experiments

Plant care and transplanting

We germinated 5,880 *BCMA* CFR-NILs under greenhouse conditions (as described above) and transplanted germinants into 98-cell "cone-tainer" racks containing ~100 mL of potting soil per 3.8 cm diameter cone (Steuwe & Sons, Inc., Tangent, OR). In the greenhouse, we assigned racks to three treatments with different starting frequencies of the *MM* genotype: high = 66% *MM*, mid = 50% *MM*, and low = 34% *MM*. Individuals were assigned to random positions within racks. We shipped racks overnight to the Rocky Mountain Biological Laboratory and arranged 10 racks (3 high, 4 mid, and 3 low f(*MM*)) in a random configuration in each of the six array sites. Replicate individuals of each CFR-NIL genotype spanned multiple independent family lines to control for possible effects of unlinked loci outside of the *BCMA1/3* region.

To facilitate insect access to arrays, we sunk each rack flush with the soil and surrounding neighbor vegetation by digging a separate rectangular hole for each rack, and excluded megaherbivores with wire cages. Because plants in racks were confined to a relatively small volume of soil, we watered all arrays twice per week for the first two weeks of the experiment. Despite this, plants began to show signs of drought stress (wilting, browning of leaves; **Figure 3A**); thus, we watered all arrays every other day for the duration of the 2016 growing season. After 8 weeks, we removed the arrays from the field, scored them for survival and herbivore damage (described above), and terminated the experiment.

Field measurements

We measured survival and herbivore damage on array plants as described above for garden transplants.

Variation in herbivore resistance and survival across environments

We tested for differences in the effects of *BCMA1/3* alleles on survival and herbivore defense across environments using the general approach described above for garden transplants; however, because we manipulated starting genotype frequencies in the arrays, our statistical models also included fixed effects of genotype frequency and the *BCMA1/3* × frequency interaction, in addition to other fixed and random effects described above.

Frequency-dependent effects

We tested for frequency-dependent effects of *BCMA1/3* alleles by assessing the significance of the frequency and *BCM1/3* × frequency model effects for herbivore resistance and survival using Type III Wald tests, Kenward-Roger tests, and parametric bootstrapping, as described above (**Supplementary Tables 1A and 3A**).

Response to selection

We assessed array-level trends in genotype frequency changes as a test for response to drought-mediated selection in our array experiment, in which plants showed signs of drought stress (**Figure 3A**). To do so, we calculated the final frequency of the *MM* genotype within each array as follows:

$$Final\ f(MM) = \frac{final\ MM}{(final\ MM + final\ BB)}$$

and the proportion mortality per array as follows:

$$Mortality = 1 - \frac{(final\ MM + final\ BB)}{(initial\ MM + initial\ BB)}$$

for each of the 60 arrays. We regressed the final frequency of the *MM* genotype onto the array proportion mortality, accounting for fixed effects of environment, the starting *MM* genotype frequency, and an mortality×f(*MM*) interaction, using standard least squares ANCOVA in JMP Pro v. 14.3.0.

One array (#34) was an extreme outlier for viability selection, with proportion mortality = 0.72 (all other 59 arrays: 0 – 0.45). We also assessed the effect of viability selection on genotype frequency excluding this outlier using the same methods. This outlier singlehandedly drove a significant mortality×f(*MM*) interaction, so in the main text we report the results excluding this point. Full results from both models are provided in **Supplementary Table 5**. The qualitative conclusion of both models is the same: the frequency of the *MM* genotype increased with greater mortality due to drought.

Greenhouse drought experiments

CFR-NIL dry-down

Plant care and experimental setup

We implemented a progressive dry-down experiment (*sensu* Mojica et al. 2016) to gradually induce drought stress in *BCMA1/3* CFR-NIL genotypes. We germinated 1,000 CFR-NIL seedlings in petri dishes and transplanted them into 2" × 2" square pots. The 1,000 individuals included 100 replicate individuals for each of five family lines within each *BCMA3* genotype, half of which were randomly assigned to a drought treatment. We assigned each pot to a position in one of 32 greenhouse flats using a completely randomized design, such that each rack contained replicated individuals of multiple family lines per genotype, some of which were assigned to each experimental treatment.

We transplanted germinants into pots with known masses of fritted clay potting medium (Profile® Greens Grade™ Porous Ceramic; mean clay mass = 34.35 ± 0.16 g per pot). Fritted clay absorbs and releases water more evenly than potting soil, and the relationship between volumetric water content (VWC) and water potential (Ψ_W) is well-characterized in this substrate (van Bavel et al. 1978, Mojica et al. 2016). We grew germinants under well-watered conditions for six weeks until juvenile plants were established. Because fritted clay is an inorganic substrate that is chemically inert, we saturated pots with 0.5x strength Hoagland's solution prior to transplanting germinants, and then again twice weekly until beginning the drought treatment. Growth conditions in the Duke University greenhouse included a 16h day with minimum light levels 600μmol/cm^2, and temperatures ranging 18.3-21.1° C daily / 15.0-17.7° C nightly.

Controlled drought treatment

For individuals assigned to the drought treatment, after the 6-week growth period, we began withholding water to induce drought stress. Specifically, we weighed each pot in the dry treatment daily and divided the current weight by the saturated weight (measured for each pot prior to transplanting) to calculate the current percent saturation for each individual *i* as follows:

$$\%\ sat_i = \frac{current\ mass_i}{saturated\ mass_i}$$

After weighing all pots in the drought treatment, we identified the individual in the experiment with the highest percent saturation (max(% sat)), and watered every other pot *i* with the volume of water required to achieve an equal saturation to the wettest pot, as follows:

$$volume\ to\ add_i = (\max(\%\ sat) * sat\ mass_i) - (\%\ sat_i * sat\ mass_i)$$

In this way, we gradually reduced the substrate VWC (and thus water potential) over the span of several days, drying down the plants gradually and allowing them to respond morphologically and physiologically to drought conditions. Throughout the span of the drought treatment, plants in the wet treatment were watered to saturation daily by flooding greenhouse benches with water for 30 min.

Plant measurements and data analysis

We ceased the dry-down after 12 days, when the plants in the dry treatment had begun to wilt, and measured a variety of morphological phenotypes on all individuals: height (length of the longest leaf), total leaf number, number of green leaves, leaf width, and growth rate (final

height – starting height / length of experiment). In addition, we estimated three physiological traits, including leaf water content (LWC):

$$LWC = \frac{rosette\ fresh\ weight - rosette\ dry\ weight}{rosette\ fresh\ weight}$$

leaf mass per area (LMA):

$$LMA = \frac{longest\ leaf\ dry\ mass}{longest\ leaf\ length * longest\ leaf\ width}$$

and daily water use for each day:

$$water\ use_t = final\ mass_{t-1} - initial\ mass_t$$

where the final mass is the mass following watering on day *t*-1, and the initial mass is the mass prior to watering on day *t*. For the latter, we then calculated the least squares mean values of daily water use per individual by regressing the mass of water used per day onto day number, including a random effect of individual plant to account for repeated measures on the same individuals over time, using a restricted maximum likelihood linear mixed effects model in JMP Pro v. 14.3.0. For tissue measurements, we obtained fresh weights immediately following the completion of the experiment, and dry weights from samples dried at room temperature for a minimum of 6 months.

We used data from all plants (wet and dry treatments) to test for effects of *BCMA1/3* on drought response. Specifically, we used linear mixed-effects models ('lmer' function in the 'lme4' package) to fit each measured phenotype in response to *BCMA1/3,* drought treatment, and the *BCMA* × drought interaction, as well as starting height as a fixed covariate and random effects of block and family line (**Supplementary Table 6**). We estimated least-squares mean and standard error values for each genotype in each treatment from these models using the 'emmeans' package v. 1.5.0 (Lenth 2020). We tested the significance of fixed effects in each model using Type III Wald chi-square tests with the 'Anova' function in the 'car' package v. 3.0-9 (Fox & Weisberg 2019). If our models detected a significant genotype × treatment effect, we assessed pairwise differences across all categories using a Tukey HSD post-hoc test. We tested the significance of random effects using likelihood ratio tests, comparing the full model to nested, reduced models containing single-term deletions of each random effect.

For plants in the drought treatment, we analyzed variation in water use with linear mixed effects models ('lmer' function) in the 'lme4' package v. 1.1-21. We fit least-squares mean daily water use in response to the fixed effect of one other phenotype, *BCMA1/3,* and the *BCMA1/3* × phenotype interaction, as well as random effects of greenhouse block and family line (**Supplementary Table 7A-C**). (In one model using final height as the phenotypic predictor of interest, we also included starting height as a fixed covariate.) We tested the significance of fixed effects using Type III Wald chi-square tests with the 'Anova' function in the 'car' package v. 3.0-9 (Fox & Weisberg 2019). We tested the significance of random effects using likelihood ratio tests, as described above.

For morphological variables which were significant in these individual models, we fit a multivariate model assessing variation in water use in response to *BCMA1/3* and all morphological predictors, as well as random effects of block and family line, using 'lme4' (**Supplementary Table 7D**). As above, we tested for significance of fixed effects using Type III Wald chi-square tests using 'car'. We tested the significance or random effects using likelihood ratio tests, as described above. All CFR-NIL drought response analyses run in R were performed using R v. 4.0.2 (R Core Team 2020).

Dry-down with broad panel of accessions

Plant care and experimental setup

To test for pleiotropic effects of *BCMA1/3* on drought response in variable genetic backgrounds, we performed an additional controlled greenhouse dry-down experiment (methods as described above for the *BCMA1/3* CFR-NIL genotypes, with modifications). We grew 6 biological replicates of each of 350 accessions collected from across the species range in a randomized complete block design in the greenhouse. These accessions largely overlap with the panel of genotypes used to determine range-wide variation in glucosinolate profile (see above and **Figure 1**). We used three greenhouse benches as complete blocks, each containing 700 individuals, which spanned the 350 genotypes and two treatments (wet and dry). We grew plants for 8 weeks (vs. 6 weeks for CFR-NILs) prior to initiating the drought treatment. The progressive dry-down was implemented as described above, and terminated when all pots reached 40% VWC.

Plant measurements and data analysis

Following the dry-down, 1,283 individuals representing 315 accessions survived. We harvested the full rosette from each plant to measure its fresh weight and dry weight, the latter measured after drying tissue in a drying oven at 65°C for one week. We used these measurements to calculate leaf water content (LWC) per individual plant as described above for *BCMA1/3* CFR-NILs. To estimate the least-squares mean LWC per accession, we used a REML generalized linear mixed model, treating accession, block, and the accession × drought treatment interaction as random effects, and the main effect of treatment as a fixed effect. We calculated genotypic least squares means in JMP v. 12 (SAS Institute, Cary, NC, USA).

Next, to test for genetic covariance among LWC and BC-ratio, we regressed genetic mean LWC under drought upon the genetic mean BC-ratio for each accession using linear models ('lm' in R). In three parallel models, we compared alternative statistical approaches to controlling for population structure (**Supplementary Table 8**). In approach A, we included a categorical fixed effect of genetic group (*sensu* Wang et al. 2019). In approach B, we instead used principal component axes 1-5 describing genomic variation across the full panel of accessions (*sensu* Wang et al. 2019). In approach C, we performed a separate genomic principal components analysis as in B (*sensu* Wang et al. 2019), but focusing on a subset of 132 accessions from the COL+UTA genetic groups, which have high genetic variation (Wang et al. 2019) and low LD around *BCMA3* (**Figure 4C**). In all cases, we tested the significance of fixed effects in the model using Type III ANOVA using 'car' v. 3.0-9 (Fox & Weisberg 2019). The total sample sizes retained in these models (**Supplementary Table 8**) reflect the accessions which had been included in the dry-down experiment, had been phenotyped for BC-ratio, and met the following approach-specific criteria: had been assigned to a genetic group in Wang et al. 2019 (approach A), had been included in the range-wide genomic PCA in Wang et al. 2019 (approach B), or belonged to population group COL or UTA and was included in the new genomic PCA on this subset of accessions (approach C).

Phenotype-environment correlations

Natural selection by abiotic factors may result in phenotype-environment correlations, in which the trait responding to selection is correlated with the selective driver across the landscape

(Lee & Mitchell-Olds 2011; The 1,001 Genomes Consortium 2016; Anderson & Wadgymar 2020). With a panel of 283 accessions from across the species range, we tested for past selection on GS profile in *B. stricta* using phenotype-environment associations.

First, we used each accession's location of origin to extract 19 bioclimatic variables from WorldClim (http://www.worldclim.org/bioclim). We reduced correlated axes of climate variation using principal components analysis (PCA) in JMP Pro v14.3.0 and extracting multivariate climatic coordinates for each accession in PC space up to the 5th PC axis, summarizing >90% of climate variation (**Supplementary Table 10**).

We used linear models ('lm' in 'stats'; R v.4.0.2; R Core Team 2020) to fit BC-ratio in response to latitude, longitude, elevation of origin, and five principal component axes of climate variation (all fixed effects). Accounting for population structure using three different approaches (A, B, and C, as described above in models testing for genetic correlations among traits), we identified significant climatic predictors of BC-ratio (**Supplementary Table 9**) using Type III ANOVA ('car'; Fox & Weisberg 2019), and used axis loading (**Supplementary Table 10**) to determine which raw climate variables contributed to the most significant multivariate axes. We then fit reduced linear models assessing variation in BC-ratio in response to each of these raw climate variables, controlling for population structure using approaches A, B, and C described above (**Supplementary Table 11**). In all of these models, because residuals of linear models were non-normally distributed, we used permutation tests to assess the significance of each climate effect on BC-ratio. Specifically, we randomly reshuffled BC-ratio values (thus maintaining the relationship between climate and population structure) 10,000 times without replacement for each linear model. We then compared the observed *F*-statistic for each climate variable to the distribution of permuted *F*-statistics for the same climate variables, and calculated the one-sided *P*-value as 1 minus the percentile in which the observed *F*-statistic fell in the empirical cumulative distribution function for the permuted values.

Dissecting the *BCMA3* region

Assembly of the B. stricta *version_2 reference genome*

Initial characterization of possible linked loci in the *BCMA* region using the version_1 *B. stricta* reference genome (Lee et al. 2017) was unsatisfactory. The version_1 reference genome was constructed from the LTM genotype, which contains at least two tandem copies on chromosome 7 (*BCMA1* and *BCMA3*), as well as other repetitive elements (see "Evolutionary history of *BCMA3*" in Main Text and Supplementary Methods); alignment of new reads to this region yielded poor consensus sequences. To resolve ambiguity about the identity of nearby loci in the *BCMA3* region, we assembled two version_2 *B. stricta* reference genomes using long-read sequencing technology with the Montana (LTM) and the Colorado (SAD) accessions. Full details of resolution of repetitive elements, characterization of the *BCMA* haplotype, etc. following genome assembly are described below in "Evolutionary history of *BCMA1/3* duplications".

Sample materials

We spread seeds from focal *B. stricta* genotypes (LTM [MT] and SAD12 [CO]) in 55 mm petri dishes with 2 pieces of filter paper immersed in ddH_2O and stored them at 4° C until

germination. We transplanted germinants into potting soil and grew them in a growth chamber set to 22° C with a 16 h day length.

High molecular weight DNA extraction

For the LTM (MT) genotype, we extracted DNA according to Mayjonade et al. (2018) with some modifications. Briefly, we ground ~3.5 g of etiolated young leaves to powder in liquid N_2. We added lysis buffer containing RNAse A (Qiagen, 100 mg/mL) to tissue powder and incubated at 50° C for 30 minutes. We then added 5 M potassium acetate equal to 1/3 the lysis buffer volume. We mixed these solutions, incubated the mixture at 4° C for 30 minutes, and centrifuged tubes at 5,000 g for 10 min. We added one volume of phenol:chloroform:isoamyl alcohol (25:24:1, v/v, Thermo Fisher, USA) to the clarified supernatant. We inverted the solutions and centrifuged tubes at 8,000 g for 15 minutes, twice. We collected the supernatants and added one volume of binding buffer containing pre-washed Ampure beads (Beckman Coulter, USA) to each tube. We incubated these mixtures for 10 minutes, placed the tubes on a magnet, and removed the supernatant. We then washed the Ampure beads with 70% ethanol. Subsequently, we added 100 μL TE buffer (pH 8.0) to the mixture, and incubated tubes at 37° C for 20 minutes. Finally, we placed tubes on a magnet for 1 h and eluted high molecular weight DNA in 1x TAE buffer.

For the SAD12 (CO) genotype, viscous metabolites hampered DNA extraction, so we used a modified extraction approach. First, we isolated nuclei according to Gendrel et al. (2005). We then filtered supernatants through pre-equilibrated anion exchange tips (Genomic-tip 20/G, Qiagen, USA), and performed subsequent extraction steps according to the manufacturer's instructions. Finally, we dissolved high-molecular-weight DNA in TE buffer (pH 8.0).

Library preparation and sequencing

We end-repaired genomic DNA using NEBNext FFPE Repair Mix and NEBNext End repair / dA-tailing Module (New England Biolabs, Ipswich, MA, USA), and then ligated sequencing adapters using NEBNext Quick Ligation Module (New England Biolabs), adapter mix and ligation buffer (SQK-LSK109 Ligation Sequencing Kit 1D, ONT, England). We cleaned library mixtures using 0.4x volume of AmPure beads (Beckmann Coulter, USA) and eluted cleaned libraries into 15 µl of elution buffer (SQK-LSK109). We performed Oxford Nanopore Technology (ONT) MinION sequencing according to the manufacturer's guidelines using R9 flow cells (FLO-MIN106, ONT). We performed base calling using Guppy v2.3.5 (available on ONT community website, https://community.nanoporetech.com).

Genome assembly and quality evaluation

We removed adapters from the raw sequencing file with Porechop (https://github.com/rrwick/Porechop). We then used the correction function in Canu (Koren et al. 2017) to correct high-noise Nanopore sequences. For LTM (MT) and SAD12 (CO), reads shorter than 1 kb and 3 kb, respectively, were filtered out in this correction step. Next, we assembled reads into contigs using Smartdenovo (https://github.com/ruanjue/smartdenovo) with the k-mer ranging from 16 to 31. We assessed assembly quality using Quast (Mikheenko et al. 2018), and selected the genome assembly with the lowest contig number and highest N50 value for further analyses. We polished the best-quality assembly using Pilon (Walker et al. 2014) with the Illumina reads generated previously (NCBI Sequence Read Archive SRR396758).

Genome annotation

We used both transcriptome-based and *ab initio* prediction for genome annotation. We downloaded paired-end RNAseq reads of *B. stricta* LTM (MT) from JGI (JGI Project ID: 405127). We used HISAT2 (Kim et al. 2015) to align the transcriptome to the polished LTM (MT) Nanopore genome, and used StringTie (Pertea et al. 2015) to perform reference-based transcriptome assembly. We imported the assembled transcriptome into TransDecoder (Haas et al. 2013) to predict candidate coding regions with UniProt (UniProt Consortium 2019) as a reference. For *ab initio* prediction, we used AUGUSTUS (Stanke & Morgenstern 2005) to predict genes directly from the reference genome. We imported all results into EVidenceModeler (Haas et al. 2008) to obtain a weighted consensus gene structure. We searched the final annotation against the UniProt database by using Blast2GO (Götz et al. 2008). According to BUSCO, the completeness of the annotation was 96.5% (LTM (MT) genome v2.0) (Samão et al. 2015).

Repeat analysis and genome comparison

We performed *de novo* repeat identification in both LTM (MT) and SAD12 (CO) genomes. We constructed a repeat library using RepeatModeler (Smit & Hubley 2015) and RepBase (Bao et al. 2015), and annotated the repeats in the combined repeat library with RepeatMasker (Smit et al. 2018).

To compare the assembly of *B. stricta* reference genomes version_2 and version_1.2 (Lee et al. 2017), we first broke the version_1.2 scaffolds at positions with single or multiple nucleotide N. Those long sequences (now without nucleotide N) were then treated as "long reads" and mapped onto the version_2 genome with minimap2 (Li 2018). The region of the version_2 genome not covered by the version_1.2 reads therefore represented locations that were either not assembled or treated as nucleotide N in the version_1.2 genome.

To identify rRNA gene locations, we downloaded *Arabidopsis thaliana* 5S (AJ307346.2) and 35S (X52320.1) rDNA from GenBank and performed blast search against the v2.2 genome.

Ordering and orienting scaffolds into linkage groups

In order to group scaffolds of LTM (MT) into chromosomes, we downloaded Illumina paired-end reads of 199 LTM (MT) × SAD12 (CO) recombinant inbred lines (RILs) from NCBI Sequence Read Archive (NCBI Sequence Read Archive SRR3947175-SRR3947373). We trimmed low-quality bases using Trimmomatic (Bolger et al. 2014) and mapped paired-end reads to the version_2 LTM (MT) genome (contigs only, at this stage) with the Burrows-Wheeler Aligner (Li & Durbin 2009), We used the Genome Analysis Toolkit (Van der Auwera et al. 2013) to create a variant call format (vcf) file containing both parents and 199 RILs. We used VCFtools (Danecek et al. 2011) to filter out indels and non-biallelic SNPs, and then filtered and transformed the vcf file as described in Lee et al. (2017). Briefly, SNPs were filtered by their depth and nucleotide calls, polarized as parental alleles, and the "marker genotype" of each 100 kb-window was determined by the proportion of parental reads in the window, resulting in LTM (MT) homozygote, SAD12 (CO) homozygote, and heterozygote windows. Also, during this process, several RILs with high heterozygosity (likely due to sample contamination) were removed, leaving 179 RILs left for further analyses. Next, the genotype table was imported into MSTmap (Wu et al. 2008) to build a genetic linkage map, resulting in seven linkage groups. Finally, the output of MSTmap was imported into ALLMAPS (Tang et al. 2015) to connect scaffolds into chromosomes.

Final versions and publication

We used the Oxford Nanopore long read technology to assemble new reference genomes of *Boechera stricta* accessions LTM (MT) and SAD12 (CO). A total of four Nanopore flow cells were used for LTM, generating 31.4 Gb of data. After quality filtering, adaptor sequence removal, and excluding reads shorter than 1 kb, 25.8 Gb of data (approximately 140-fold of the genome) in 5.9 M reads with N50 at 15.3 kb were used for assembly. The genome was assembled into about 190 Mb, with 34 contigs and a BUSCO score at 98.5% (Supplementary Table 21). Almost all of the assembly (189 Mb) was successfully placed on seven chromosomes using linkage map information, with the entire chromosome 4 assembled into one contig (utg4). While the total assembly size was similar between this version_2 and the previous version_1.2 (Lee et al. 2017), genome version_1.2 contains 12.9% of nucleotide N (**Supplementary Table 15**), reducing the assembly size with informative nucleotides down to 164.84 Mb. On the other hand, none of our 190-Mb LTM genome contains nucleotide N (except the gaps separating contigs), and almost all of the assembly can be placed on chromosomes.

Further, we generated three versions of the assembly. Genome version_2.0 contains the original 34 contigs without chromosome information. Genome version_2.1 connected 27 contigs (some with known location but uncertain orientation on chromosomes) into chromosomes, and kept the 7 other scaffolds independent. Genome version_2.2 connected 19 contigs with well-supported location and orientation into chromosomes, while keeping the 15 other contigs independent. We performed gene and repeat annotation for all three versions. In total, the annotation pipeline incorporating both *ab initio* prediction and RNAseq evidence predicted 38,328 genes in genome version_2.0, with 26,002 of them having BLAST hits in the Uniprot protein database. After the LTM genome was finalized (version_2.2), we connected the SAD12 contigs into chromosomes by aligning them to the LTM chromosomes while accounting for a known chromosomal inversion in chromosome 1 (Lee et al. 2017).

Finalized, new reference genome assemblies (version_2.2) and raw Nanopore reads for SAD12 and LTM accessions were submitted to NCBI (BioProject number PRJNA609209).

Characterizing the CFR-NIL segregating region

Genotyping-by-sequencing

With a new high-quality genome to use as a reference, we characterized genetic variation within the *BCMA1/3* region using genotyping-by-sequencing. Specifically, we grew 67 *BCMA* CFR-NILs (34 *BB* homozygotes and 33 *MM* homozygotes spanning 23 independent family lines) in potting soil under standard greenhouse conditions (as described above in "Characterizing GS variation") for approximately 2 months, until rosettes were well established. We harvested ~100 mg leaf tissue from each individuals after keeping plants in the dark for 2 days to promote carbohydrate breakdown, and stored tissue at -80° C until processing. We ground frozen leaf tissue at high speed using a Geno/Grinder® automated tissue homogenizer and cell lyser (Spex® Sample Prep, Metuchen, NJ, USA) and extracted genomic DNA using a DNeasy® Plant Mini Kit (Qiagen® N.V., Hilden, Germany) according to the manufacturer's instructions. We used extracted DNA to prepare genomic libraries for sequencing according to Andolfatto et al. (2011), with some modifications (Perera 2019), as follows.

We digested 10μL of 2ng/μL DNA with 0.6 μL of MSE1 restriction enzyme (stock concentration; New England Biolabs) in 2 μL of NEB Buffer 4 (New England Biolabs) with 0.2 μL of bovine serum albumen (stock concentration; New England Biolabs) and 7.2 μL ddH_2O,

totaling 10 µL per reaction per sample. We incubated the digestion for 3h at 37° C and then 20 min at 65° C. We added unique adaptor sequences to each sample by adding 10µL of digested genomic DNA to 8µL of 5µM adapter solution along with 0.2µL T4 DNA Ligase (400U), 5µL T4 DNA Ligase buffer, and 22.8µL ddH_2O, totaling 46µL per sample. We incubated these mixtures at 16° C for 3h to ligate adapters to the sheared genomic fragments. We pooled uniquely identified samples, concentrated, cleaned, and resuspended DNA according to Andolfatto et al. 2011. We size-selected genomic fragments ranging from ~250-300 bp in length using a 2% agarose gel with 1x TAE buffer and a GeneRuler 50bp DNA ladder (ThermoFisher Scientific). We purified excised agarose bands using a QiaQuick Gel Extraction Kit (Qiagen® N.V., Hilden, Germany) according to the manufacturer's instructions.

Finally, we added GBS indexed primers and amplified genomic fragments using PCR. Specifically, we mixed 2µL of purified, size-selected library DNA with 12.5µL Phusion® High Fidelity PCR Mastermix (New England Biolabs) 1.25µL 10µM indexed FC1 primer, 1.25µL 10µM indexed FC2 primer, and 8µL of ddH_2O. We used the following PCR protocol: hot start for 30s at 98° C; 15 cycles of 10s at 98° C, 15s at 60° C, and 15s at 72° C; and final extension for 7 min at 72° C. We purified the PCR products using Ampure XP PCR purification beads (Beckman Coulter Life Sciences) according to the manufacturer's instructions, and in the final step eluted DNA into 30µL of TE buffer. We measured the final concentration of each library using a Qubit™ dsDNA HS Assay Kit according to the manufacturer's instructions, and adjusted the concentrations of the libraries to 10 nM as necessary using ddH_2O. We sequenced the GBS libraries using the Illumina HiSeq 4000 platform (150 bp paired-end reads) at the Duke University Sequencing and Genomic Technologies Shared Resource center.

Data processing

We demultiplexed sequence reads using fastq-multx with default settings (https://github.com/brwnj/fastq-multx) and aligned them to the *Boechera stricta* version_2 reference genome (see above) using the Burrows-Wheeler Aligner (BWA; Li 2013). We called SNPs using GATK as described in Wang et al. (2019), assigning genotype values of -1, 0, 1, and 2 for missing, homozygous for the reference allele, heterozygous, and homozygous for the alternative allele, respectively. We aligned GBS sequence reads to the version_2 reference, which was constructed from the SAD12 (CO) genotype, so reference alleles reflect those derived from the SAD12 (Met-GS) CFR-NIL parent and alternate alleles reflect those derived from the LTM (BC-GS) CFR-NIL parent (see "Assembly of the *B. stricta* version_2 reference genome" above).

SNP filtering

We filtered aligned SNP data to focus on chromosome 7, where the *BCMA1/3* polymorphism is located. After filtering to remove two samples with few or low quality reads, indels, sites with mean read depth >20 (to exclude repetitive regions), sites with missing data at a frequency > 0.9, and sites with >2 alleles, we retained 3,580 SNPs among 65 CFR-NIL individuals.

F_{ST} analysis

To determine the physical size of the variable interval in the CFR-NILs, we calculated F_{ST} according to Wang et al. (2019) between the sequenced *MM* and *BB* homozygotes in 20 kb non-overlapping windows along chromosome 7. We used BLAST to locate the position of the *BCMA3* gene within this region.

Identifying flanking genes

Using the denovo version_2 LTM assembly, we identified all genes falling within 250 kb of the high-F_{ST} *BCMA1/3* CFR-NIL interval. We identified putatively functional genes from this list (which may include transposons) using BLAST against the *Arabidopsis thaliana* reference genome (The Arabidopsis Information Resource [TAIR] 2020]; Berardini et al. 2015). We then used BLAST to map *A. thaliana* genes back to the version_2 SAD12 reference, to determine the distance between flanking genes and *BCMA1/3*. We used the version_2 SAD12 reference to determine the location of flanking genes because it is annotated, and was the reference used for F_{ST} (above) and linkage disequilibrium (below) analyses. We determined putative function of *A. thaliana* orthologs by searching the TAIR database (The Arabidopsis Information Resource 2020), and associated literature, to determine whether or not genes other than *BCMA1/3* may contribute to any phenotypes characterized in this study.

***Linkage disequilibrium near* BCMA1/3**

We used *B. stricta* genotypes from the COL and UTA genetic groups, which have the greatest genetic variation (Wang et al. 2019). Using published sequence data from these accessions, we aligned Illumina reads to the SAD12 version_2 reference genome using BWA (Li 2013), and called SNPs using GATK following Wang et al. (2019). We located the *BCMA3* gene in the version_2 reference using BLAST; it spans positions 11,779 – 11,782 kb. We also located the limits of the non-recombinant *BCMA1/3* haplotype using F_{ST} analysis (above), which spans from 11,737 – 11,949 kb. We analyzed LD among SNPs within 250 kb of this interval, spanning 11,487kb – 12,199 kb on chromosome 7. We calculated LD among SNPs with minor allele frequency > 0.05 and missing rate < 0.6 in three groups of accessions: (1) the 157 COL genotypes in the subset, (2) the 126 UTA genotypes in the subset, and (3) full panel of 283 COL+UTA genotypes. We implemented all other SNP filtering thresholds as described in Wang et al. (2019). These methods retained 2,229 SNPs in the COL group (1), 2,131 SNPs in the UTA group (2), and 2,460 SNPs in the COL+UTA group (3). To characterize the general extent of LD around *BCMA*, we estimated LD (r^2) between each pair of SNPs within the 712 kb interval using *PLINK* (Purcell et al. 2007) (**Figure 4C**). Our filtering thresholds retained one SNP within the *BCMA3* gene (minor allele frequency = 0.21, missing rate = 0.28).

Polymorphism in BCMA3

Because GBS data did not resolve the complete sequence of *BCMA3,* we used Sanger sequencing to gain an in-depth understanding of genetic variation influencing glucosinolate profiles. Specifically, we Sanger sequenced the *BCMA3* gene in a panel of 110 genotypes, a stratified random sample spanning all genetic groups from the full genotype panel described in Wang et al. (2019) (**Supplementary Table 16**).

We reared all plants and extracted DNA from these 110 genotypes as described in Prasad et al. (2012). Using genomic DNA templates, we used primers targeting *BCMA3* but not *BCMA1* to amplify the gene of interest (**Supplementary Table 17**) following Prasad et al. (2012). Before sequencing, we treated PCR products with shrimp alkaline phosphatase (rSAP; New England Biolabs) and *E. coli* exonuclease I (New England Biolabs), each at a concentration of 0.5 uL per 5 mL of PCR product. We sequenced purified amplicons using standard Sanger sequencing methods at Eton Bioscience, Inc. (San Diego, CA, USA).

We trimmed raw reads using Sequencher® v. 5.3 standard end trimming criteria. For the 5' end, reads were trimmed no more than 25% until the first 25 bases contained fewer than 3 ambiguities and fewer than 3 bases with confidence <25. For the 3' end, starting at 100 bases after the 5' trim end, we trimmed the first 25 bases containing more than 3 ambiguities. In addition, we trimmed the 3' end reads until the last 25 bases contained fewer than 3 ambiguities and fewer than 3 bases with confidence <25. On both ends of the reads, any ambiguous bases were removed. We aligned trimmed reads to published *BCMA3* gene sequences from mRNA (Prasad et al. 2012; NCBI accessions JQ337907 [LTM accession] and JQ337909 [SAD12 accession]). Some intron sequences were incomplete, so introns were excised from the aligned sequences. We used this trimmed, aligned data to call SNPs in *BCMA3* (see "Molecular signatures of selection", below).

Visually inspecting the 110 aligned sequences, we observed two major structural variants: an 8bp deletion and a premature stop codon. We used custom R code to identify which genotypes contained the 8bp deletion, and the location of the deletion in the alignment, in nt. We then used grep to remove gaps from the aligned DNA sequence, allowing the 8bp deletion to disrupt the reading frame of *BCMA3*, as would be the case during *in situ* translation. We used the Biostrings package (Pagès et al. 2020) in R to translate the gapless *BCMA3* sequences using the standard genetic code. We used custom R code to identify the presence of stop codons (coded as "*") and their location in the translated amino acid sequence. Assuming no alternative splicing patterns in *BCMA3*, we replaced all translated codons following the first stop codon with "*". Finally, we parsed the translated amino acid sequences by position, focusing on amino acid residues in positions 148 and 268, which are hypothesized to cause differential glucosinolate biosynthesis among SAD12 and LTM genotypes, with mutations L148V and V268M associated with BC-GS biosynthesis in LTM (Prasad et al. 2012).

We used linear models to test how structural genetic variation and molecular variation in the *BCMA3* amino acid sequence influence BC-ratio. Because structural genetic variants and amino acid variants were confounded (**Supplementary Table 18**), we used a suite of linear models to test the effect of each variant on BC-ratio separately, controlling for genetic group (**Supplementary Table 12**). To test the effect of structural genetic variation on BC-ratio, we modeled BC-ratio in response to fixed effects of genetic group, exon length (full length vs. premature stop), and 8bp deletion (present vs. absent). To test the effect of amino acid substitutions on BC-ratio, we modeled BC-ratio in response to fixed effects of genetic group and molecular phenotype (concatenated amino acid residues at positions 148 and 268 in the BCMA3 enzyme). For the model testing effects of amino acid substitutions, we further subsetted the data to focus on genotypes lacking the premature stop codons (N=69) to specifically test for the effects of amino acid residues in complete BCMA3 enzymes. We tested the significance of effects in both models using Type III ANOVA (car::Anova(, type=3); Fox & Weisberg 2019).

In our surveyed accessions, we revealed further genetic variation in the *BCMA3* locus than had been previously described (Prasad et al. 2012) (**Supplementary Table 18**). All

accessions containing the 8bp deletion (N=20) had a frame-shift in the translated amino acid sequence causing a premature stop codon. This deletion began at nucleotide position 371 in all 20 accessions, causing the premature stop codon at position 137 in the amino acid sequence, before either amino acid residue of interest (148 or 268) is expressed. An additional three accessions had premature stop codons in *BCMA3* not caused by a frame-shift 8bp deletion. In two of these accessions, the premature stop occurred at position 287 in the amino acid sequence, and in the third, it occurred in position 313. In all three of these genotypes, the premature stop occurred after both amino acid residues of interest. The predicted full length of the BCMA3 enzyme is 541 amino acids. Among full-length alleles, we also observed additional variation in critical amino acid residues; in addition to L148/V268 and V148/M268 variants, which correspond to the molecular phenotypes of the SAD12 and LTM genotypes, respectively, 58% of full-length alleles contained V148/V268 residues.

Interestingly, structural genetic variation in *BCMA3*, but not amino acid substitutions at hypothesized critical BCMA3 residues, predicted variation in BC-ratio (**Supplementary Table 12**). The presence of premature stop codons in any position is associated with low-BC ratio (**Figure 5A**). Among full-length alleles, BC-ratio varies across BCMA3 molecular phenotypes as hypothesized in Prasad et al. (2012) (**Figure 5A**), but differences in BC-ratio across groups are not statistically significant (**Supplementary Table 12**).

Evolutionary history of *BCMA1/3* duplications

New long-read assemblies of both CFR-NIL parents, LTM (MT) and SAD12 (CO), revealed substantial variation in the number of *BCMA* copies present in the CFR-NIL haplotype (**Extended Data Figure 7**). While the CO parent has a single copy of *BCMA* (*BCMA3*) on chromosome 7, the *BCMA3* region in the MT parent is rich in transposons and tandem repeats, containing two functional copies of *BCMA* (*BCMA1* and *BCMA3*) and at least ten non-functional duplicated pseudogenes. We used phylogenetic reconstruction to infer the evolutionary history of these duplication events and the evolution of functional allelic variation. We used MEGA7 (Kumar et al. 2016) to construct a phylogenetic tree of version_2 genome sequences of *BCMA* copies in the LTM and SAD12 genotypes, with 1,000 bootstrap resamplings using the maximum likelihood algorithm. We used the general time reversible nucleotide substitution model, allowing invariant sites and a gamma distribution allow evolution rate differences among sites.

To precisely characterize *BCMA* copy number variation in the parents of the CFR-NILs, we searched the *BCMA3* gene sequence (GenBank JQ337907) against the LTM (MT) and SAD12 (CO) genomes using BLAST+ (Camacho et al. 2009) and drew dot plots of the *BCMA1/3* region (**Extended Data Figure 7**) using Gepard (Krumsiek et al. 2007).

We also assessed natural variation in *BCMA* copy number across sequenced accessions (157 COL accessions, 105 NOR accessions, 126 UTA accessions, 81 WES accessions and 17 admixed genotypes) (Wang et al. 2019) to investigate the copy number of *BCMA* in natural *B. stricta* populations. We downloaded all of the SRA numbers archived from Wang et al. (2019b) as well as SRA number SRR396758 for the MT (LTM) accession. To ensure that all *BCMA*-related reads were mapped onto the *BCMA3* copy in the CO accession, we created a new "reference" genome by masking ± 10 kb region of *BCMA2* in the CO genome. We mapped the whole genome sequences of 486 accessions to the *BCMA2*-masked reference genome with BWA after cutting adapters and checking quality (Li & Durbin 2009, Martin 2011). We used samtools to calculate the read depth of the *BCMA3* gene with mapping quality > 30 for each accession (Li 2011). We then divided the *BCMA3* sequencing depth of each accession by that accession's genome-wide average sequencing depth, excluding repetitive regions identified previously; this

yields a "read depth ratio" to estimate copy number of all *BCMA* genes. Because SAD12 (CO) is known to have only a single copy of *BCMA* on chromosome 7 (*BCMA3*) in addition to the single copy on chromosome 2 (*BCMA2*) (Prasad et al. 2012), we expect SAD12 to have a read depth ratio of approximately 2 according to this analysis.

Using phylogenetic reconstruction, we inferred the evolutionary history of *BCMA3* alleles and gene copies (**Extended Data Figure 5**), which read depth ratio analysis revealed to be variable among genotypes **(Supplementary Figure 1**). We found that, following the divergence of the genera *Boechera* and *Arabidopsis*, the *BCMA2* gene on chromosome 2 (orthologous to *CYP79F1/2* in *Arabidopsis*) duplicated, yielding the ancestor of *BCMA1/3* on chromosome 7. Further, a sister species within the genus, *B. retrofracta*, has only a single copy of *BCMA1/3*, and is a sequence outgroup to all *B. stricta* paralogs on chromosome 7. This gene phylogeny suggests that the duplication of *BCMA1/3* occurred within *B. stricta* following divergence from *B. retrofracta*. Finally, the reconstruction demonstrates that duplication of the functionally divergent *BCMA1* and *BCMA3* copies (Prasad et al. 2012) occurred prior to differentiation between the two *B. stricta* subspecies, represented by the MT and CO parents (Lee et al. 2017, Wang et al. 2019), indicating that there was a secondary loss of *BCMA1* from the ancestor of the CO parental genotype (**Supplementary Figure 2**). Thus, functional differentiation among *BCMA3* alleles evolved within the *B. stricta* species. This suggests that the BC-ratio polymorphism has since increased to intermediate frequencies within *B. stricta*, possibly due to balancing selection favoring multiple functional variants, rather than incomplete lineage sorting of ancestral polymorphisms.

Molecular signatures of selection

The presence of gene duplications (see above) caused low mapping quality of resequencing data to the *BCMA* region; misaligning Illumina reads from *BCMA* paralogs onto *BCMA3* could artificially inflate estimates of nucleotide diversity in this gene. Thus, we used Sanger sequencing to target *BCMA3* when testing for molecular signatures of selection.

Beginning with aligned Sanger sequence data on the *BCMA3* locus in 110 genotypes across the species range (see "Polymorphism in *BCMA3*"), we focused on a subset of 54 genotypes belonging to the COL and UTA genetic groups (Wang et al. 2019). We excluded sequence data for genotypes from other genetic groups because of residual population structure within WES and low BC-ratio variation within NOR. We also excluded one genotype from the COL group that was previously excluded from analyses in Wang et al. (2019). We called SNPs in the aligned panel of sequences assuming that all sequenced regions were homozygous, given the high inbreeding rate in *B. stricta* (Song et al. 2009); indeed, no loci within *BCMA3* appeared to be heterozygous, so this assumption did not alter any data processing. Some of these *BCMA3* sequences were supported by only a single read, which could introduce rare sequencing or Taq errors. To correct for this, we identified single-read regions, comprising 42.8% of the Sanger data. We reasoned that possible sequencing errors would occur as singletons in the data set, so we assigned any singleton SNPs in the single-read regions to the more common allele. (Only seven such changes were made in the total Sanger data set.)

Following these corrections, we calculated π among the 364 silent sites in *BCMA3* among the 54 genotypes using DnaSP v6.12.03. We then calculated π among fourfold sites in other comparable genes in the genome, using the same 54 genotypes. Beginning with all genes in the

genome, we chose high-quality Illumina-based sequences fulfilling three criteria: (A) $\pi > 0$, (B) number of silent sites > 360, and (C) excluding regions known to be influenced by historical balancing selection (~10% of the genome; Wang et al. 2019). We implemented criterion A to exclude genes for which sequence data was missing or of low quality, precluding estimation of π. We implemented criterion B to account for the effect of gene length on π (**Supplementary Figure 3**). We implemented criterion C to test for molecular signatures of selection in *BCMA3* in comparison to regions of the genome that do not show broad signals of balancing selection. (*BCMA3* does not fall in the regions showing historical balancing selection in Wang et al. 2019.) Our filtering retained 1,689 genes. Before calculating π in other genes, we randomly selected 42.8% of the filtered dataset and "corrected" singleton SNPs in these regions to the common allele. This allowed us to compare polymorphism in *BCMA3* to the genome-wide distribution despite different sequencing methods for the *BCMA3* gene (this study) and other genes in the genome (Wang et al. 2019).

We compared the observed value of π_{BCMA} to the genome-wide distribution of π for comparable loci among our 54 focal genotypes. We determined whether π_{BCMA} was a statistical outlier by comparing its value to the cutoff of the 5% upper tail of π values in the subset of comparable genes.

Effect size of the *BCMA1/3* locus

We estimated the average effect of the *BCMA1/3* polymorphism on herbivore damage in nature. In each common garden field environment, we calculated the mean herbivore damage (percent leaf area removed) for the two homozygous CFR-NIL genotypes. We calculated the effect size of *BCMA1/3* on herbivore damage as the absolute value of the difference in CFR-NIL means within each environment, divided by the standard deviation of herbivore damage (across all individuals) in that environment. (This is the difference in damage levels between *BCMA1/3* homozygotes, scaled in phenotypic standard deviation units.) The *BCMA1/3* polymorphism explained an average of 0.1715 standard deviations of herbivore damage across transplant environments, ranging from 0.0126 standard deviations in MAH-2014 to 0.4330 standard deviations in GTH-2016.

References appearing in the Supplementary Information

The 1001 Genomes Consortium. 1,135 Genomes Reveal the Global Pattern of Polymorphism in *Arabidopsis thaliana*. *Cell* **166,** 1–11 (2016).

Anderson, J. T. & Wadgymar, S. M. Climate change disrupts local adaptation and favours upslope migration. *Ecology Letters* **23,** 181–192 (2020).

The Arabidopsis Information Resource Center (TAIR). arabidopsis.org (2020).

Bates, D., Maechler, M., Bolker, B. & Walker, S. Fitting linear mixed-effects models using lme4. *Journal of Statistical Software* **67,** 1–48 (2015).

Berardini, T. Z. *et al.* The Arabidopsis Information Resource: Making and mining the "gold standard" annotated reference plant genome. *genesis* **53,** 474-485 (2015).

Camacho, C. *et al.* BLAST+: architecture and applications. *BMC Bioinformatics* **10,** 421 (2009).

Crone, E. E. Is survivorship a better fitness surrogate than fecundity? *Evolution* **55,** 2611–2614 (2001).

Fox, J. & Weisberg, S. *An {R} Companion to Applied Regression, Third Edition.* Sage Publications, Thousand Oaks CA (2019).

Hadfield, J. D. Estimating evolutionary parameters when viability selection is operating. *Proceedings of the Royal Society of London B: Biological Sciences* **275,** 723–734 (2008).

Halekoh, U. & Højsgaard, S. A Kenward-Roger approximation and parametric bootstrap methods for tests in linear mixed models - the R package pbkrtest. *Journal of Statistical Software* **59,** 1–30 (2014).

Kahle, D. & Wickham, H. ggmap: Spatial visualization with ggplot2. *The R Journal* **5,** 144–161 (2013).

Krumsiek, J., Arnold, R. & Rattei, T. Gepard: a rapid and sensitive tool for creating dotplots on genomic scale. *Bioinformatics* **23,** 1026–1028 (2007).

Kumar, S., Stecher, G. & Tamura K. MEGA7: Molecular Evolutionary Genetics Analysis version 7.0 for bigger datasets. *Molecular Biology and Evolution* **33,** 1870–1874 (2016).

Lee, C.-R. & Mitchell-Olds, T. Quantifying effects of environmental and geographical factors on patterns of genetic differentiation. *Molecular Ecology* **20,** 4631–4642 (2011).

Lee, C.-R. *et al.* Young inversion with multiple linked QTLs under selection in a hybrid zone. *Nature Ecology and Evolution* **1,** 1–11 (2017).

Lenth, R. emmeans: Estimated Marginal Means, aka Least-Squares Means. R package version 1.3.4 (2019).

Li, H. Aligning sequence reads, clone sequences and assembly contigs with BWA-MEM. Preprint at https://arxiv.org/abs/1303.3997 (2013).

Mayjonade, B. *et al.* Extraction of high-molecular-weight genomic DNA for long-read sequencing of single molecules. *BioTechniques* **61,** 203–205 (2018).

Mojica, J. P., & Kelly, J. K. Viability selection prior to trait expression is an essential component of natural selection. *Proceedings of the Royal Society B: Biological Sciences* **277,** 2945–2950 (2010).

Mojica, J. P. *et al.* (2016) Genetics of water use physiology in locally adapted *Arabidopsis thaliana*. *Plant Science* **251,** 12–22.

Pagès, H., Aboyoun, P., Gentleman, R., & DebRoy, S. Biostrings: efficient manipulation of biological strings. R package version 2.56.0 (2020).

Perera, N. S. *Repeated Evolution of Asexuality Among Hybrids of a Recently Diverged Subspecies Pair in Boechera.* Dissertation, Duke University (2019).

Prasad, K. V. S. K. *et al.* A gain-of-function polymorphism controlling complex traits and fitness in nature. *Science* **337,** 1081–1084 (2012).

R Core Team. R: A language and environment for statistical computing. R Foundation for Statistical Computing, Vienna, Austria. https://www.R-project.org/ (2020).

Schluter, D., Price, T. D. & Locke, R. Conflicting selection pressures and life history trade-offs. *Proceedings of the Royal Society of London B: Biological Sciences* **246**: 11–17 (1991).

Schranz, M. E., Manzaneda, A. J., Windsor, A. J., Clauss, M. J. & Mitchell-Olds, T. ecological genomics of *Boechera stricta*: Identification of a QTL controlling the allocation of methionine- vs branched-chain amino acid-derived glucosinolates and levels of insect herbivory. *Heredity* **102,** 465–474 (2009).

Sønderby, I. E., Geu-Flores, F. & Halkier, B. A. Biosynthesis of glucosinolates – gene discovery and beyond. *Trends in Plant Science* **15,** 283–290 (2010).

Song, B.-H. *et al.* Multilocus patterns of nucleotide diversity, population structure, and linkage disequilibrium in *Boechera stricta,* a wild relative of Arabidopsis. *Genetics* **181,** 1021-1033 (2009).

van Bavel, C. H. M., Lascano, R. & Wilson, D. R. Water relations of fritted clay. *Soil Science Society of America Journal* **42,** 657–659 (1978).

928 Wadgymar, S. M., Dawes, S. C. & Anderson, J. T. Integrating viability and fecundity selection
929 to illuminate the adaptive nature of genetic clines. *Evolution Letters* **1,** 26–39 (2017).
930
931 Wagner, M. R., & Mitchell-Olds, T. Plasticity of plant defense and its evolutionary implications
932 in wild populations of *Boechera stricta*. *Evolution* **72,** 1034–1049 (2018).
933
934 Wang, B., *et al.* Ancient polymorphisms contribute to genome-wide variation by long-term
935 balancing selection and divergent sorting in *Boechera stricta*. *Genome Biology* **20,** 126
936 (2019).
937
938 Wang, B., *et al.* Correction to: Ancient polymorphisms contribute to genome-wide variation by
939 long-term balancing selection and divergent sorting in *Boechera stricta*. *Genome Biology*
940 **20,** 161. (2019b)
941
942 Windsor, A. J. *et al.* Geographic and evolutionary diversification of glucosinolates among near
943 relatives of *Arabidopsis thaliana* (Brassicaceae). *Phytochemistry* **66,** 1321–1333 (2005).